# Structure and Properties of $[Fe_4S_4\{2,6\text{-bis(acylamino)benzenethiolato-}S\}_4]^{2-}$ and $[Fe_2S_2\{2,6\text{-bis(acylamino)benzenethiolato-}S\}_4]^{2-}$: Protection of the Fe−S Bond by Double NH···S Hydrogen Bonds

**Norikazu Ueyama,* Yusuke Yamada, Taka-aki Okamura, Shuuji Kimura, and Akira Nakamura***

Department of Macromolecular Science, Faculty of Science, Osaka University, Toyonaka, Osaka 560, Japan

*Received April 19, 1996*[⊗]

Iron−sulfur clusters containing a singly or doubly NH···S hydrogen-bonded arenethiolate ligand, $[Fe_4S_4(S\text{-}2\text{-}RCONHC_6H_4)_4]^{2-}$ (R = $CH_3$, *t*-Bu, $CF_3$), $[Fe_4S_4\{S\text{-}2,6\text{-}(RCONH)_2C_6H_3\}_4]^{2-}$, $[Fe_2S_2(S\text{-}2\text{-}RCONHC_6H_4)_4]^{2-}$ (R = $CH_3$, *t*-Bu, $CF_3$), and $[Fe_2S_2\{S\text{-}2,6\text{-}(RCONH)_2C_6H_3\}_4]^{2-}$, were synthesized as models of bacterial [4Fe-4S] and plant-type [2Fe-2S] ferredoxins. The X-ray structures and IR spectra of $(PPh_4)_2[Fe_4S_4\{S\text{-}2,6\text{-}(CH_3CONH)_2C_6H_3\}_4]\cdot 2CH_3CN$ and $(NEt_4)_2[Fe_2S_2\{S\text{-}2,6\text{-}(t\text{-}BuCONH)_2C_6H_3\}_4]$ indicate that the two amide NH groups at the *o*,*o*′-positions are directed to the thiolate sulfur atom and form double NH···S hydrogen bonds. The NH···S hydrogen bond contributes to the positive shift of the redox potential of not only $(Fe_4S_4)^{+}/(Fe_4S_4)^{2+}$ but also $(Fe_4S_4)^{2+}/(Fe_4S_4)^{3+}$ in the [4Fe-4S] clusters as well as $(Fe_2S_2)^{2+}/(Fe_2S_2)^{3+}$ in the [2Fe-2S] clusters. The doubly NH···S hydrogen-bonded thiolate ligand effectively prevents the ligand exchange reaction by benzenethiol because the two amide NH groups stabilize the thiolate by protection from dissociation.

## Introduction

The crystallographic analysis of *Peptococcus aerogenes*[1] and *Bacillus thermoproteolyticus* [4Fe-4S] ferredoxins[2] has also revealed the presence of two kinds of the NH···S hydrogen bonds. One is a single NH···S hydrogen bond between one amide NH group and a thiolate, and other is a double NH···S hydrogen bond between two amide NH groups and a thiolate as shown in Figure 1a. Their presence has been proposed by the close location (ca. 3 Å) between amide N and sulfur atoms.

The redox potentials of $(Fe_4S_4)^{2+}$ ferredoxin model complexes with alkane- and arenethiolate ligands have been extensively studied by Holm and his co-workers.[3,4] They have found that the redox potential is regulated not only by the dielectric constant of the solvent but also by the electronic properties of the *p*-substituent of the arenethiolate ligands.[3] Actually, they demonstrated the positive shift of the redox potential by the electron-withdrawing group of the *p*-substituted benzenethiolate ligand.

The chemical role of the NH···S hydrogen bonds on the redox potential has been verified using ferredoxin model [4Fe-4S] peptide complexes[5,6] and tripeptide-like model complexes.[7] It has been emphasized that the NH···S hydrogen bond is supported in a low dielectric constant solvent, e.g, dichloromethane or 1,2-dimethoxyethane, in contrast to the general tendency of the positive shift by a solvent having a high dielectric constant[8] or large donor number.[9]

On the other hand, native [4Fe-4S] ferredoxins have far more positive-shifted redox potential (−524 to −694 mV vs SCE) than those of the model complexes[10] even though there is no electron-withdrawing substituent in the protein. Native ferredoxins have been proposed to regulate the redox potential using the electrostatic environments created by the specific combination of amino acid residues and solvent or by the formation of a specific intramolecular NH···S hydrogen bond.[11]

As for the above [4Fe-4S] ferredoxins, the presence of an NH···S hydrogen bond in the active center of plant-type [2Fe-2S] ferredoxins, functioning by a similar electron transfer,[12] has also been proposed by the X-ray crystal structure,[13,14] $^1$H-NMR spectroscopic,[15] and resonance Raman spectroscopic analyses.[16] Most of the single NH···S hydrogen bonds and the double NH···S hydrogen bonds converge on one of the two Fe(III) ions in the active center of the *Spirulina platensis* [2Fe-2S] ferredoxin shown in Figure 1b.[13,17] One of the proposed roles for the NH···S hydrogen bond in these [2Fe-2S] ferredoxins is also considered to shift the redox potential to the positive side.

Synthetic model complexes having alkane- and arenethiolate ligands have been synthesized, e.g., $[Fe_2S_2(S_2\text{-}o\text{-}xyl)_2]^{2-}$ ($S_2$-

[⊗] Abstract published in *Advance ACS Abstracts,* October 1, 1996.

(1) Adman, E. T.; Sieker, L. C.; Jensen, L. H. *J. Biol. Chem.* **1976**, *251*, 3801.
(2) Fukuyama, K.; Nagahara, Y.; Tsukihara, T.; Katsube, Y.; Hase, T.; Matsubara, H. *J. Mol. Biol.* **1988**, *199*, 183.
(3) DePamphilis, B. V.; Averill, B. A.; Herskovitz, T.; Que, L., Jr.; Holm, R. H. *J. Am. Chem. Soc.* **1974**, *96*, 4159.
(4) Hill, C. L.; Renaud, J.; Holm, R. H.; Mortenson, L. E. *J. Am. Chem. Soc.* **1977**, *99*, 2549.
(5) Ueyama, N.; Terakawa, T.; Nakata, M.; Nakamura, A. *J. Am. Chem. Soc.* **1983**, *105*, 7098.
(6) Ueyama, N.; Kajiwara, A.; Terakawa, T.; Ueno, S.; Nakamura, A. *Inorg. Chem.* **1985**, *24*, 4700.
(7) Ohno, R.; Ueyama, N.; Nakamura, A. *Inorg. Chem.* **1991**, *30*, 4887.
(8) Kassner, R. J.; Yang, W. *J. Am. Chem. Soc.* **1977**, *99*, 4351.
(9) Blonk, H. L.; Roelofsen, A. M.; Frelink, T.; Anders, M. J.; Schmitz, J. E. J.; Linden, J. G. M. v. d.; Steggerda, J. J. *J. Phys. Chem.* **1992**, *96*, 6004.
(10) Berg, J. M.; Holm, R. H. In *Metal Ions in Biology*; Spiro, T. G., Ed.; Wiley-Interscience: New York, 1982; p 1.
(11) Carter, C. W. *J. Biol. Chem.* **1977**, *252*, 7802.
(12) Orme-Johnson, W. H. *Annu. Rev. Biochem.* **1973**, *42*, 159.
(13) Tsukihara, T.; Fukuyama, K.; Nakamura, M.; Katsube, Y.; Kanaka, N.; Kakudo, M.; Hase, T.; Wada, K.; Matsubara, H. *J. Biochem.* **1981**, *90*, 1763.
(14) Correll, C. C.; Batie, C. J.; Ballou, D. P.; Ludwig, M. L. *Science* **1992**, *258*, 1604.
(15) Dugad, L. B.; Mar, G. N. L.; Banci, L.; Bertini, I. *Biochemistry* **1990**, *29*, 2263.
(16) Sanders-Loehr, J. *Metal Clusters in Proteins*; American Chemical Society: Washington, DC, 1988; p 49.
(17) Fukuyama, K.; Hase, T.; Matsumoto, S.; Tsukihara, T.; Katsube, Y.; Tanaka, N.; Kakudo, M.; Wada, K.; Matsubara, H. *Nature* **1980**, *286*, 522.

S0020-1669(96)00432-6 CCC: $12.00 

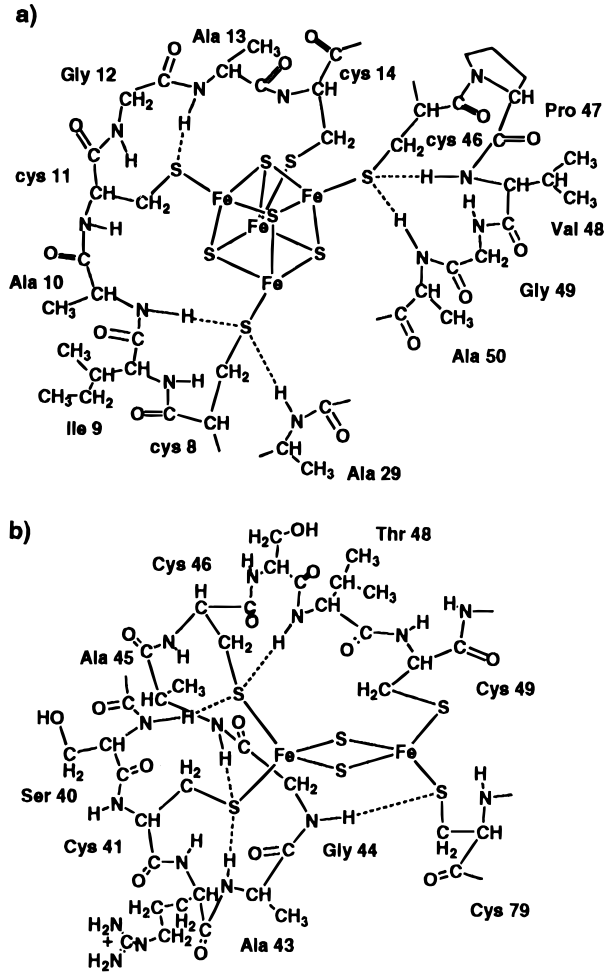


**Figure 1.** Single and double NH···S hydrogen bonds observed in the active centers of (a) *P. aerogenes* [4Fe-4S] ferredoxin[1] and (b) *S. platensis* [2Fe-2S] ferredoxin.[17]

*o*-xyl= *o*-xylene-α,α′-dithiolato),[18] $[Fe_2S_2(S\text{-}p\text{-}MeC_6H_4)_4]^{2-}$, and $[Fe_2S_2(SC_6H_5)_4]^{2-}$,[19] and their chemical properties were characterized thoroughly. Furthermore, chelating peptide model complexes exhibited a more positively shifted redox potential than that of the simple alkane- or arenethiolate model complexes.[20] The preferably chelating peptide ligand presumably affords a specific intramolecular NH···S hydrogen bond. A specially designed 20-peptide complex with all amino acid residues adjacent to the [2Fe-2S] active center of the *S. platensis* ferredoxin has exhibited a positive-shifted redox potential relative to that of the native ferredoxin with NH···S hydrogen bonds.[21]

This paper presents our recent observations not only on the positive shift of redox potential but also on other chemical functions of the NH···S hydrogen bond using various simple 2-mono(acylamino)- and 2,6-bis(acylamino)benzenethiolate ligands as models of the active center of bacterial [4Fe-4S] and plant-type [2Fe-2S] ferredoxins. The ligands were designed with the consideration of parallel orientation of the two amide dipoles toward the sulfur atom without self-association as shown in Scheme 1. Another advantage is that an extremely bulky group can be easily introduced into the ligand by the amide formation. Thus, when ferredoxin model complexes with a novel bulky thiolate having an intramolecular NH···S hydrogen bond are constructed, the hydrogen bond is strengthened by the surrounding groups just as the hydrophobic amino acid residues in native ferredoxins.

**Scheme 1**

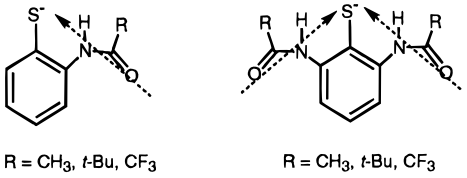


## Experimental Section

All procedures were performed in argon atmosphere by the Schlenk technique. All solvents were dried over calcium hydride and distilled under argon before use.

$(NEt_4)_2[Fe_4S_4(SPh)_4]$[3] and $(NEt_4)_2[Fe_4S_4(S\text{-}2,4,6\text{-}i\text{-}Pr_3C_6H_2)_4]$[22] were prepared by the reported method. $(NEt_4)_2[Fe_2S_2(SC_6H_5)_4]$ was prepared by the reported method.[3,18] 2,2′-Dithiobis(*N*-phenyl-2,2-dimethylpropanamide), bis{2,6-bis(acetylamino)phenyl} disulfide, bis{2,6-bis((trifluoroacetyl)amino)phenyl} disulfide, and bis{2,6-bis(pivaloylamino)phenyl} disulfide were synthesized by literature methods.[23]

**Synthesis of $(NEt_4)_2[Fe_4S_4(S\text{-}2\text{-}CH_3CONHC_6H_4)_4]$ (1a).** The complex was synthesized by the ligand exchange method. A mixture of $(NEt_4)_2[Fe_4S_4(SPh)_4]$ (175 mg, 0.17 mmol) and bis(2-(acetylamino)-phenyl) disulfide (119 mg, 0.36 mmol) in acetonitrile (3 mL) was stirred at room temperature for 24 h. The solution was concentrated under reduced pressure. The black precipitate was recrystallized from acetonitrile/diethyl ether and washed with diethyl ether. The black microcrystals were collected and dried under reduced pressure. Yield: 110 mg (52%). $^1$H-NMR (acetonitrile-$d_3$): $\delta$ (ppm) amide NH, 8.28 (s 1H), 6-H, 7.91 (s 1H), 4-H, 7.84 (s 1H), 3-H, 6.54 (s 1H), 5-H, 5.83 (s 1H), $CH_3$ (s 3H). FAB-MS (*m*/*z*): 1276.1 (calcd 1276.5 for $(Et_4N)_2[Fe_4S_4(S\text{-}2\text{-}CH_3CONHC_6H_4)_4]^-$), 1145.8 (calcd 1145.9 for $(Et_4N)[Fe_4S_4(S\text{-}2\text{-}CH_3CONHC_6H_4)_4]^-$). Anal. Calcd for $C_{48}H_{72}Fe_4N_6O_4S_8$: C, 45.16; H, 5.69; N, 6.58. Found: C, 44.54; H, 5.71; N, 6.29.

**Synthesis of $(NEt_4)_2[Fe_4S_4(S\text{-}2\text{-}t\text{-}BuCONHC_6H_4)_4]$ (2a).** The compound was synthesized by the same method as that used for **1a**. A mixture of $(NEt_4)_2[Fe_4S_4(SPh)_4]$ (175 mg, 0.17 mmol) and bis(2-(pivaloylamino)phenyl) disulfide (183 mg, 0.44 mmol) in acetonitrile (3 mL) was stirred at room temperature for 90 min. The solution was concentrated under reduced pressure. The black precipitate was recrystallized from acetonitrile/diethyl ether and washed with diethyl ether. The black microcrystals were collected and dried under reduced pressure. Yield: 177 mg (73%). $^1$H-NMR (acetonitrile-$d_3$): $\delta$ (ppm) amide NH, 8.35 (s 1H), 6-H, 9.37 (s 1H), 4-H, 7.86 (s 1H), 3-H, 6.44 (s 1H), 5-H, 5.79 (s 1H), *t*-Bu (s 9H). FAB-MS (*m*/*z*): 1444.7 (calcd 1444.3 for $(Et_4N)_2[Fe_4S_4(S\text{-}2\text{-}t\text{-}BuCONHC_6H_4)_4]^-$). Anal. Calcd for $C_{60}H_{96}Fe_4N_6O_4S_8$: C, 49.86; H, 6.69; N, 5.81. Found: C, 49.14; H, 6.59; N, 5.68.

**Synthesis of $(NEt_4)_2[Fe_4S_4(S\text{-}2\text{-}CF_3CONHC_6H_4)_4]$ (3a).** The compound was synthesized by the same method as described for **1a**. A mixture of $(NEt_4)_2[Fe_4S_4(SPh)_4]$ (157 mg, 0.15 mmol) and bis(2-((trifluoroacetyl)amino)phenyl) disulfide (153 mg, 0.35 mmol) in acetonitrile (3 mL) was stirred at room temperature for 90 min. The solution was concentrated under reduced pressure. The black precipitate was recrystallized from ethyl acetate/*n*-hexane and washed with *n*-hexane. The black microcrystals were collected and dried under reduced pressure. Yield: 118 mg (53%). $^1$H-NMR (acetonitrile-$d_3$): $\delta$ (ppm) amide NH and 6-H, 9.17 (br 2H), 4-H, 7.95 (s 1H), 3-H, 6.50 (s 1H), 5-H, 5.87 (s 1H). FAB-MS (*m*/*z*): 1490.7 (calcd 1492 for

(18) Mayerle, J. J.; Denmark, S. E.; Depamphilis, B. V.; Ibers, J. A.; Holm, R. H. *J. Am. Chem. Soc.* **1975**, *97*, 1032.
(19) Bobrik, M. A.; Hodgson, K. O.; Holm, R. H. *J. Am. Chem. Soc.* **1977**, *16*, 1851.
(20) Ueno, S.; Ueyama, N.; Nakamura, A. *Inorg. Chem.* **1986**, *25*, 1000.
(21) Ueyama, N.; Ueno, S.; Nakamura, A.; Wada, K.; Matsubara, H.; Kumagai, S.; Sakakibara, S.; Tsukihara, T. *Biopolymers* **1992**, *32*, 1535.
(22) Ueyama, N.; Terakawa, T.; Sugawara, T.; Fuji, M.; Nakamura, A. *Chem. Lett.* **1984**, 1287.
(23) Ueyama, N.; Taniuchi, K.; Okamura, T.; Nakamura, A.; Maeda, H.; Emura, S. *Inorg. Chem.* **1996**, *35*, 1945.

$(Et_4N)_2[Fe_4S_4(S\text{-}2\text{-}CF_3CONHC_6H_4)_4]^-$). Anal. Calcd for $C_{48}H_{60}F_{12}Fe_4N_6O_4S_8$: C, 38.63; H, 4.05; N, 5.63. Found: C, 38.82; H, 4.15; N, 5.53.

**Synthesis of $(PPh_4)_2[Fe_4S_4\{S\text{-}2,6\text{-}(CH_3CONH)_2C_6H_3\}_4]\cdot 2CH_3CN$ (1b).** $(PPh_4)_2[Fe_4S_4(SPh)_4]$ (94 mg, 64 mmol) was mixed with bis{2,6-bis(acetylamino)phenyl} disulfide (68 mg, 138 mmol) in acetonitrile (10 mL) at room temperature. After being stirred for 4 h, the solution was concentrated. To the residue was added 3 mL of diethyl ether to give black crystals after 2 days. Yield: 87 mg (67%). $^1$H-NMR (acetonitrile-$d_3$): $\delta$ (ppm) amide NH, 8.23 (br 2H), *m*-H, 9.04 (d 2H), *p*-H, 6.10 (t 1H), $CH_3$ 2.24 (s 6H). FAB-MS (*m*/*z*): 1583.2 (calcd 1583.0 for $(Ph_4P)[Fe_4S_4\{S\text{-}2,6\text{-}(CH_3CONH)_2C_6H_4\}_4]^-$). The crystal contains two acetonitrile molecules. Anal. Calcd for $C_{88}H_{84}Fe_4N_8O_8S_8P_2\cdot 2CH_3CN$: C, 55.09; H, 4.52; N, 6.98. Found: C, 56.11; H, 4.56; N, 6.99.

**Synthesis of $(NEt_4)_2[Fe_4S_4\{S\text{-}2,6\text{-}(t\text{-}BuCONH)_2C_6H_3\}_4]$ (2b).** $(NEt_4)_2[Fe_4S_4(SPh)_4]$ (66 mg, 68 mmol) was mixed with bis{2,6-bis(pivaloylamino)phenyl} disulfide (100 mg, 163 mmol) in acetonitrile (5 mL) at room temperature. After being stirred for 22 h, the solution was concentrated to give a residue. The residue was washed several times with 5 mL of diethyl ether. The crude materials were recrystallized from acetonitrile/diethyl ether and gave black crystals. Yield: 50 mg (40%). $^1$H-NMR (acetonitrile-$d_3$): $\delta$ (ppm) amide NH, 8.34 (br 2H), *m*-H, 9.20 (d 2H), *p*-H, 6.11 (t 1H), *t*-Bu 1.35 (s 18H). FAB-MS (*m*/*z*): 1710.4 (calcd 1710.4 for $(Et_4N)[Fe_4S_4\{S\text{-}2,6\text{-}(t\text{-}BuCONH)_2C_6H_4\}_4]^-$). Anal. Calcd for $C_{80}H_{132}Fe_4N_{10}O_8S_8$: C, 52.17; H, 7.22; N, 7.60. Found: C, 51.80; H, 7.16; N, 7.56.

**Synthesis of $(NMe_4)_2[Fe_4S_4\{S\text{-}2,6\text{-}(CF_3CONH)_2C_6H_3\}_4]$ (3b).** $(NMe_4)_2[Fe_4S_4(S\text{-}t\text{-}Bu)_4]\cdot CH_3CN$ (123 mg, 0.136 mmol) was mixed with bis{2,6-bis((trifluoroacetyl)amino)phenyl} disulfide (217 mg, 0.327 mmol) in acetonitrile (10 mL) at room temperature. After being stirred for 10 h, the solution was concentrated to give a residue. After being washed with 10 ml of diethyl ether several times, the residue was recrystallized from acetonitrile/diethyl ether to give black crystals. Yield: 239 mg (96%). $^1$H-NMR (acetonitrile-$d_3$): $\delta$ (ppm) amide NH, 9.28 (br 2H), *m*-H, 9.03 (d 2H), *p*-H, 6.34 (t 1H). FAB-MS (*m*/*z*): 1750.1 (calcd 1749.7 for $(Me_4N)[Fe_4S_4\{S\text{-}2,6\text{-}(CF_3CONH)_2C_6H_4\}_4]\}^-$). Anal. Calcd for $C_{52}H_{50}N_{12}O_8S_8F_{24}Fe_4$: C, 31.59; H, 2.43; N, 7.68. Found: C, 31.51; H, 2.41; N, 7.75.

**Synthesis of $(NEt_4)_2[Fe_2S_2(S\text{-}2\text{-}CH_3CONHC_6H_4)_4]$ (4a).** The complex was synthesized by a ligand exchange method. A mixture of $(NEt_4)_2[Fe_2S_2(SC_6H_5)_4]$ (270 mg, 0.31 mmol) and bis(2-(acetylamino)-phenyl) disulfide (210 mg, 0.64 mmol) in acetonitrile (10 mL) was stirred at room temperature for 1 h. The solution was concentrated under reduced pressure. The black precipitate was washed with diethyl ether and recrystallized from hot $CH_3CN$. The black microcrystals were collected and dried under reduced pressure. Yield: 150 mg (47%). $^1$H NMR (acetonitrile-$d_3$): $\delta$ (ppm) 10.9 (s, 1H, ArH), 8.9 (s, 1H, ArH), 6.8 (s, 1H, amide NH), 4.6 (s, 1H, ArH), 3.4 (s, 1H, ArH). Anal. Calcd for $C_{48}H_{72}Fe_2N_6O_4S_6$: C, 52.35; H, 6.59; N, 7.63. Found: C, 51.66; H, 6.37; N, 7.45. FAB-MS (*m*/*z*): 970.1 (calcd 970.1 for $\{(NEt_4)[Fe_2S_2(S\text{-}2\text{-}CH_3CONHC_6H_4)_4]\}^-$), 506.9 (calcd 507.9 for $[Fe_2S_2(S\text{-}2\text{-}CH_3CONHC_6H_4)_2]^-$, 417.8 (calcd 420.0 for $^1/_2[Fe_2S_2(S\text{-}2\text{-}CH_3\text{-}CONHC_6H_4)_4]^{2-}$), 341.7 (calcd 341.9 for $[Fe_2S_2(S\text{-}2\text{-}CH_3CONHC_6H_4)]^-$).

**Synthesis of $(NMe_4)_2[Fe_2S_2(S\text{-}2\text{-}t\text{-}BuCONHC_6H_4)_4]$ (5a).** The compound was synthesized by the same method as described for **4a**. A mixture of $(NMe_4)_2[Fe_2S_2(SC_6H_5)_4]$ (94 mg, 0.12 mmol) and 2,2′-dithiobis(*N*-phenyl-2,2-dimethylpropanamide) (110 mg, 0.26 mmol) in acetonitrile (10 mL) was stirred at room temperature for 21 h. The solution was concentrated under reduced pressure. The black precipitate was washed with diethyl ether and recrystallized from hot acetonitrile. The black microcrystals were collected and dried under reduced pressure. Yield: 59 mg (42%). $^1$H NMR (acetonitrile-$d_3$): $\delta$ (ppm) 10.9 (s, 1H, ArH), 8.9 (s, 1H, ArH), 6.8 (s, 1H, amide NH), 4.6 (s, 1H, ArH), 3.4 (s, 1H, ArH). Anal. Calcd for $C_{52}H_{80}Fe_2N_6O_4S_6$: C, 53.98; H, 6.97; N, 7.26. Found: C, 53.89; H, 6.75; N, 7.24. FAB-MS (*m*/*z*): 1157.1 (calcd 1156.3 for $\{(NMe_4)_2[Fe_2S_2(S\text{-}2\text{-}t\text{-}BuCONHC_6H_4)_4]\}^-$).

An amide $N^2$H-substituted complex, $(NMe_4)[Fe_2S_2(S\text{-}2\text{-}t\text{-}Bu\text{-}CONHC_6H_4)_4]$, was also synthesized by a ligand exchange reaction between $(NMe_4)_2[Fe_2S_2(SC_6H_5)_4]$ and $(S\text{-}2\text{-}t\text{-}BuCON^2H\text{-}C_6H_4)_2$ in acetonitrile.

**Synthesis of $(NEt_4)_2[Fe_2S_2(S\text{-}2\text{-}CF_3CONHC_6H_4)_4]$ (6a).** The compound was synthesized by the same method as described for **4a**. A mixture of $(NEt_4)_2[Fe_2S_2(SC_6H_5)_4]$ (210 mg, 0.24 mmol) and 2,2′-dithiobis(*N*-phenyl-2,2,2-trifluoroacetamide) (210 mg, 0.49 mmol) in acetonitrile (3 mL) was stirred at room temperature for 30 min. The solution was concentrated under reduced pressure. The black precipitate was washed with diethyl ether and recrystallized from acetonitrile/diethyl ether. The black microcrystals were collected and dried under reduced pressure. Yield: 190 mg (55%). $^1$H NMR (acetonitrile-$d_3$): $\delta$ 10.9 (s, 1H, ArH), 8.9 (s, 1H, ArH), 6.8 (s, 1H, amide NH), 4.6 (s, 1H, ArH), 3.4 (s, 1H, ArH). Anal. Calcd for $C_{48}H_{60}F_{12}Fe_2N_6O_4S_6$: C, 43.77; H, 4.59; N, 6.38. Found: C, 43.78; H, 4.39; N, 6.40. FAB-MS (*m*/*z*): 1185.7 (calcd 1186.0 for $\{(NEt_4)[Fe_2S_2(S\text{-}2\text{-}CF_3\text{-}CONHC_6H_4)_4]\}^-$).

**Synthesis of $(NEt_4)_2[Fe_2S_2\{S\text{-}2,6\text{-}(CH_3CONH)_2C_6H_3\}_4]$ (4b).** A mixture of $(NEt_4)_2[Fe_2S_2(SC_6H_5)_4]$ (166 mg, 0.19 mmol) and bis(2,6-(diacetylamino)phenyl) disulfide (169 mg, 0.38 mmol) in acetonitrile (3 mL) was stirred for 30 min at room temperature. The solution was concentrated under reduced pressure. The black precipitate was washed with diethyl ether and dried under reduced pressure. Yield: 186 mg (73%). $^1$H NMR (acetonitrile-$d_3$): $\delta$ 10.9 (s, 1H, ArH), 8.9 (s, 1H, ArH), 6.8 (s, 1H, amide NH), 4.6 (s, 1H, ArH), 3.4 (s, 1H, ArH). Anal. Calcd for $C_{56}H_{84}Fe_2N_{10}O_8S_6$: C, 50.59; H, 6.37; N, 10.54. Found: C, 49.66; H, 6.37; N, 9.66. FAB-MS (*m*/*z*): 1197.9 (calcd 1198.2 for $\{(NMe_4)[Fe_2S_2\{S\text{-}2,6\text{-}(CH_3CONH)_2C_6H_3\}_4]\}^-$).

**Synthesis of $(NEt_4)_2[Fe_2S_2\{S\text{-}2,6\text{-}(t\text{-}BuCONH)_2C_6H_3\}_4]$ (5b).** The complex was synthesized by the same method as described for **1**. A mixture of $(NEt_4)_2[Fe_2S_2(SC_6H_5)_4]$ (110 mg, 0.13 mmol) and bis{2,6-bis(pivaloylamino)phenyl} disulfide (160 mg, 0.26 mmol) in acetonitrile (3 mL) was stirred at room temperature for 30 min. The solution was concentrated under reduced pressure and washed with *n*-hexane. The black microcrystals were recrystallized from acetonitrile/diethyl ether. The black crystals were collected and dried under reduced pressure. Yield: 94 mg (43%). $^1$H NMR (acetonitrile-$d_3$): $\delta$ (ppm) 10.9 (s, 1H, ArH), 8.9 (s, 1H, ArH), 6.8 (s, 1H, amide NH), 4.6 (s, 1H, ArH), 3.4 (s, 1H, ArH). Anal. Calcd for $C_{80}H_{132}Fe_2N_{10}O_8S_6$: C, 57.68; H, 7.99; N, 8.41. Found: C, 57.08; H, 7.88; N, 8.31. FAB-MS (*m*/*z*): 1534.9 (calcd 1534.6 for $\{(NEt_4)_2[Fe_2S_2\{S\text{-}2,6\text{-}(t\text{-}BuCONH)_2C_6H_3\}_4]\}^-$).

**Synthesis of $(NEt_4)_2[Fe_2S_2\{S\text{-}2,6\text{-}(CF_3CONH)_2C_6H_3\}_4]$ (6b).** A mixture of $(NEt_4)_2[Fe_2S_2(SC_6H_5)_4]$ (47 mg, 0.05 mmol) and bis{2,6-bis((trifluoroacetyl)amino)phenyl} disulfide (71 mg, 0.11 mmol) in acetonitrile (1 mL) was stirred for 20 min at room temperature. The solution was concentrated under reduced pressure and washed with *n*-hexane. The black precipitate was recrystallized from acetonitrile/diethyl ether. The black microcrystals were collected and dried under reduced pressure. Yield: 34 mg (39%). $^1$H NMR (acetonitrile-$d_3$): $\delta$ 10.9 (s, 1H, ArH), 8.9 (s, 1H, ArH), 6.8 (s, 1H, amide NH), 4.6 (s, 1H, ArH), 3.4 (s, 1H, ArH). Anal. Calcd for $C_{56}H_{60}F_{24}Fe_2N_{10}O_8S_6$: C, 38.20; H, 3.43; N, 7.96. Found: C, 38.16; H, 3.29; N, 7.89. FAB-MS (*m*/*z*): 1630.1 (calcd 1629.9 for $\{(NMe_4)[Fe_2S_2\{S\text{-}2,6\text{-}(CF_3\text{-}CONH)_2C_6H_3\}_4]\}^-$).

**Physical Measurements.** Visible spectra in solution were recorded on a Jasco Ubest-30 spectrophotometer. $^1$H NMR spectra were taken on a Jeol EX-270 spectrometer in acetonitrile-$d_3$ solution. IR spectra were recorded on a Jasco FT/IR 8300 spectrometer. Samples were prepared as KBr pellets. Electrochemical measurements were carried out using a Yanaco P-1100 instrument in acetonitrile solution that contained 0.1 M tetra-*n*-butylammonium perchlorate as a supporting electrolyte. The $E_{1/2}$ value was referenced to the SCE electrode at room temperature, and a value uncorrected for junction potential was obtained. The scanning rate was 100 mV/s. The concentrations of ferredoxin [4Fe-4S] or [2Fe-2S] model complexes were 2.5 mM in acetonitrile in the presence of 0.1 M $n$-$Bu_4NClO_4$. Mass spectrometric analysis was performed in a 3-nitrobenzyl alcohol solution as a matrix on a Jeol JMS-SX102 mass spectrometer which was operated in a negative ion mode. Ions were produced by fast atom bombardment (FAB) with a beam of 3 keV Xe atoms and accelerating voltage of 10 kV.

**X-ray Structure and Determination.** A single crystal of $(PPh_4)_2[Fe_4S_4\{S\text{-}2,6\text{-}(CH_3CONH)_2C_6H_3\}_4]\cdot 2CH_3CN$ (**1b**) or $(NEt_4)_2[Fe_4S_4\{S\text{-}2,6\text{-}(t\text{-}BuCONH)_2C_6H_3\}_4]$ (**5b**) was sealed in a glass capillary under argon atmosphere for the X-ray measurement. The X-ray measurement was performed at 23 °C on a Rigaku AFC5R diffractometer equipped with a rotating anode X-ray generator. The radiation used was Mo Kα monochromatized with graphite (0.710 69 Å). An empirical

**Table 1.** Crystal Data Collection and Refinement Data for $(PPh_4)_2[Fe_4S_4\{S\text{-}2,6\text{-}(CH_3CONH)_2C_6H_3\}_4]\cdot 2CH_3CN$ (**1b**) and $(NEt_4)_2[Fe_2S_2\{S\text{-}2,6\text{-}(t\text{-}BuCONH)_2C_6H_3\}_4]$ (**5b**)

| | **1b** | **5b** |
|---|---|---|
| chem formula | $C_{92}H_{90}O_8N_{10}P_2S_8Fe$ | $C_{80}H_{132}O_8N_{10}S_6Fe_2$ |
| fw | 2005.60 | 1666.04 |
| color | black | black, plate |
| cryst system | triclinic | orthorhombic |
| lattice params | | |
| *a* | 14.429(4) Å | 14.431(4) Å |
| *b* | 26.700(4) Å | 25.661(5) Å |
| *c* | 12.913(2) Å | 25.765(4) Å |
| α | 94.08(1) | |
| *β* | 104.95(2) | |
| *γ* | 96.70(2) | |
| *V* | 4746(1) Å$^3$ | 9541(3) Å$^3$ |
| space group | $P\bar{1}$ | *Aba*2 (No. 41) |
| *Z* | 2 | 4 |
| $D_{calc}$ | 1.403 g cm$^{-3}$ | 1.160 g cm$^{-3}$ |
| *F*(000) | 2076 | 3576.00 |
| $\mu$ (MoKα) | 8.68 cm$^{-1}$ | 4.87 cm$^{-1}$ |
| Scan type | w | $\omega-2\theta$ |
| $2\theta_{max}$ | 55.2° | 55.0° |
| no. of reflcns | tot. 22 856, unique 21 957 | tot. 4907 |
| no. of observns | 8896 ($I > 3\sigma(I)$) | 1659 ($I > 3\sigma(I)$) |
| no. of variables | 1093 | 278 |
| residual *R*, $R_w$ values[a] | 0.048, 0.052 | 0.082, 0.091 |

[a] $R = \sum||F_o| - |F_c||/\sum|F_o|$. $R_w = [\sum w(|F_o| - |F_c|)^2/\sum wF_o^2]^{1/2}$.

absorption correction was applied. The basic crystallographic parameters for **1b** and **5b** are listed in Table 1. Unit cell dimensions were refined with 25 reflections. These standard reflections were chosen and monitored with every 100 reflections and did not show any significant change. The structure was solved by direct methods and expanded using Fourier techniques. Some non-hydrogen atoms (Fe, S, O, C, N) were refined anisotropically, while the rest were refined isotropically. Hydrogen atoms were included but not refined. The final cycle of full-matrix least-squares refinement for **1b** was based on 8896 observed reflections ($I > 3.00\sigma(I)$) and 1093 variable parameters with unweighted and weighted agreement factors ($R = 0.048$, $R_w = 0.053$). The final cycle of full-matrix least-squares refinement for **5b** was based on 1659 observed reflections ($I > 3.00\sigma(I)$) and 278 variable parameters and converged (largest parameter was 2.62 times its esd) with unweighted and weighted agreement factors ($R = 0.082$, $R_w = 0.091$).

## Results

**Synthesis.** [4Fe-4S] and [2Fe-2S] ferredoxin model complexes having 2-(acylamino)- or 2,6-bis(acylamino)benzenethiolate are easily synthesized by the ligand exchange reaction from a well-established [4Fe-4S] model complex, $(NR_4)_2[Fe_4S_4(SPh)_4]$,[3,24] in the presence of an equivalent amount of disulfide as described as follows:

$$(NR_4)_2[Fe_4S_4(SPh)_4] + 2ArSSAr \xrightarrow[\text{in } CH_3CN]{} (NR_4)_2[Fe_4S_4(SAr)_4] + 2PhSSPh$$

$$(NR_4)_2[Fe_2S_2(SPh)_4] + 2ArSSAr \xrightarrow[\text{in } CH_3CN]{} (NR_4)_2[Fe_2S_2(SAr)_4] + 2PhSSPh$$

Ar = 2-(acylamino)- or 2,6-bis(acylamino)benzenethiolato

Although the reaction was expected to stop after the equilibrium was reached, the bis(2-acylamino)phenyl disulfide or bis{2,6-bis(acylamino)phenyl} disulfide was consumed completely and the exchange reaction was quantitative. Similar facile ligand exchange reaction for the synthesis of the ferredoxin model complex $(NR_4)_2[Fe_4S_4(SePh)_4]$ has been demonstrated in the reaction between $(NR_4)_2[Fe_4S_4(SPh)_4]$ and diphenyl diselenide.[24] The difference in nucleophilicity between both thiolates presumably promotes the exchange reaction. In general, the acidity of the thiolate is proportional to the oxidation potential of the thiolate.[25−27] 2-(Acylamino)- or 2,6-bis(acylamino)benzenethiol has a larger acidity than that of benzenethiol because the thiolate is stabilized with a low protonation affinity. The large acidity is not ascribed to the electronic effect of the *o*-substituent because a low Hammett constant ($\sigma_p = -0.002$) for the acetylamide group at the *p*-position of the benzene ring is known.[28] Presumably, the NH···S hydrogen bond is associated with the stabilization of the thiolate as discussed later.

The detection of $[Fe_4S_4(SAr)_4]^{2-}$ and $[Fe_2S_2(SAr)_4]^{2-}$ clusters in the [4Fe-4S] and [2Fe-2S] ferredoxin model complexes was carried out using mass spectroscopy in an acetonitrile solution. These complex anions gave mainly as doubly charged fragments of $[Fe_4S_4(SAr)_4]^{2-}$ or $[Fe_2S_2(SAr)_4]^{2-}$, similar to those of the mass-spectral pattern reported for $(NR_4)_2[Fe_4S_4(SPh)_4]$.[29]

**Crystal Structure of $(PPh_4)_2[Fe_4S_4\{S\text{-}2,6\text{-}(CH_3CONH)_2C_6H_3\}_4]\cdot 2CH_3CN$ (1b).** The structure of the anion part of complex **1b** is shown in Figure 2a. The crystal structure of $(NMe_4)_2[Fe_4S_4\{S\text{-}2,6\text{-}(CF_3CONH)_2C_6H_3\}_4]$ (**3b**) is almost the same as that of **1b** although the *R* value ($R = 0.123$, monoclinic, *C*2/c) for **3b** is relatively large. Complex **1b** crystallizes in the $P\bar{1}$ space group. **1b** contains two molecules of acetonitrile per one molecule of the cluster in the solid state. The crystal structure indicates the absence of coordination of acetonitrile molecules to the Fe ions. Table 2 lists the mean values of the selected structural parameters for **1b**. These complexes also have a $[Fe_4S_4]^{2+}$ core structure similar to that of $[Fe_4S_4(SPh)_4]^{2-}$ reported in the literature.[24] Unfortunately, we could not succeed in the crystallographic analysis of all the model complexes having a single NH···S hydrogen bond.

The structure of $[Fe_4S_4]^{2+}$ cubane in **1b** is similar to the structural parameters reported for $[Fe_4S_4(SPh)_4]^{2-}$.[24] The mean Fe−S* and Fe···Fe distances in **1b** are 2.277 and 2.726 Å, respectively, whereas the corresponding distances reported for $[Fe_4S_4(SPh)_4]^{2-}$ are 2.286 and 2.736 Å, respectively.[24] Similarly, the mean Fe−S*−Fe (73.5°) and S*−Fe−S* (104.3°) angles in **1b** are almost the same as those (73.5 and 104.3°, respectively) in $[Fe_4S_4(SPh)_4]^{2-}$.

The Fe−S bond distance for **1b** is 2.277 Å (mean) similar to that (mean, 2.263 Å) for $[Fe_4S_4(SPh)_4]^{2-}$.[24] The distance is also similar to that of 2.274 Å in $[Fe_4S_4(S\text{-}2,4,6\text{-}Me_3C_6H_2)_4]^{2-}]^{2-}$.[30] Complex **1b** exhibits Fe−S−C angles of 102.1 and 98° (means), which are relatively smaller than the value 106.1° (mean) of the reported one for $[Fe_4S_4(SPh)_4]^{2-}$.[24] The smaller Fe−S−C angle by the NH···S hydrogen bonding reflects the ionic character of the Fe−S bond.

**Crystal Structure of $(NEt_4)_2[Fe_2S_2\{S\text{-}2,6\text{-}(t\text{-}BuCONH)_2C_6H_3\}_4]$ (5b).** Complex **5b** crystallizes in the *Aba*2 space group and has a 2-fold axis at the center of the $(Fe_2S_2)^{2+}$ core. The ORTEP drawing of the anion part of **5b** is shown in Figure 2b. Table 3 lists the selected bond distances and bond angles. All amide NH groups are directed to the thiolate sulfur atoms and presumably form the double NH···S hydrogen bonds. The Fe−

(24) Que, L., Jr.; Bobrik, M. A.; Ibers, J. A.; Holm, R. H. *J. Am. Chem. Soc.* **1974**, *96*, 4168.
(25) Edward, J. O. *J. Am. Chem. Soc.* **1956**, *78*, 1819.
(26) Freter, R.; Pohl, E. R.; Wilson, J. M.; Hupe, D. J. *J. Org. Chem.* **1979**, *44*, 1771.
(27) Wilson, J. M.; Bayer, R. J.; Hupe, D. J. *J. Am. Chem. Soc.* **1977**, *99*, 7922.
(28) Jaffe, H. H. *Chem. Rev.* **1953**, *53*, 191.
(29) Lee, W. L.; Gage, D. A.; Huang, Z. H.; Chang, C. K.; Kanatzidis, M. G.; Allison, J. *J. Am. Chem. Soc.* **1992**, *114*, 7132.
(30) Ueyama, N.; Sugawara, T.; Fuji, M.; Nakamura, A.; Yasuoka, N. *Chem. Lett.* **1985**, 175.

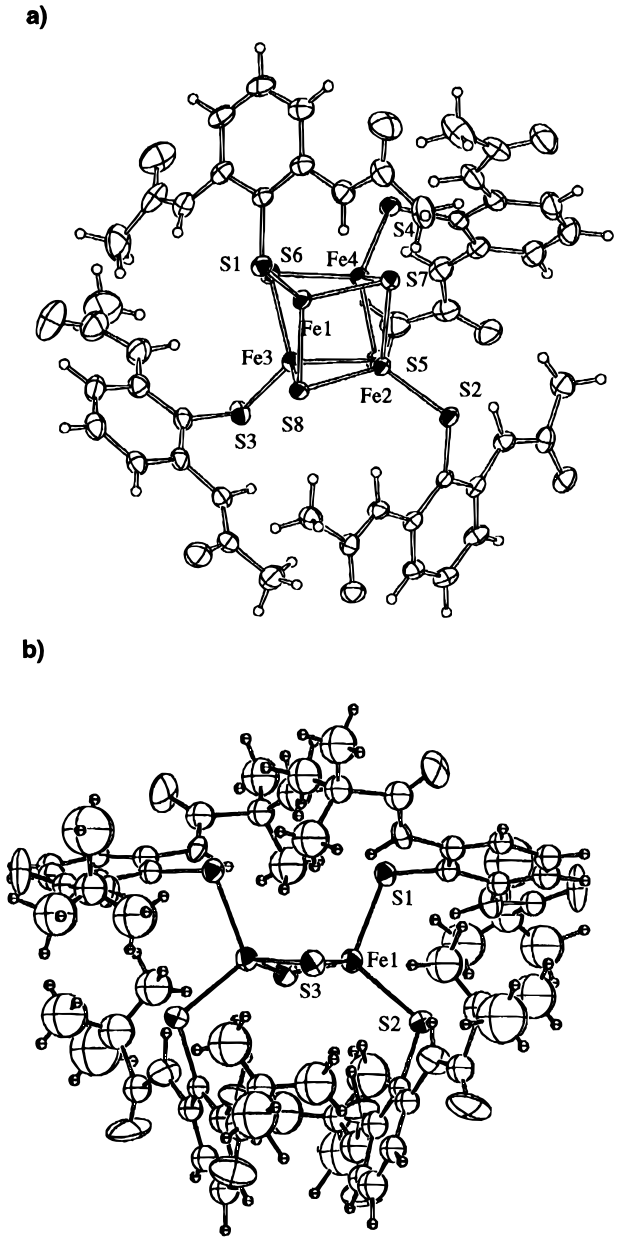


**Figure 2.** (a) ORTEP drawings of the anion parts of $(PPh_4)_2[Fe_4S_4\{S\text{-}2,6\text{-}(CH_3CONH)_2C_6H_3\}_4]\cdot 2CH_3CN$ (solvent molecules omitted for clarity). (b) ORTEP drawings of the anion parts of $(NEt_4)_2[Fe_2S_2\{S\text{-}2,6\text{-}(t\text{-}BuCONH)_2C_6H_3\}_4]$ (**5b**).

$S_{br}$ ($S_{br}$ = bridging inorganic sulfide) distances of **5b** are 2.198(7) and 2.203(7) Å similar to those of the reported model complexes, $[Fe_2S_2(S\text{-}p\text{-}MeC_6H_4)_4]^{2-}$,[18] $[Fe_2S_2(S_2\text{-}o\text{-}xyl)_2]^{2-}$,[18] and $[Fe_2S_2(tmbt)_4]^{2-}$ (tmbt = 2,4,6-trimethylbenzenethiolate).[31] The Fe−S−C atoms and the aromatic ring lie on the same plane in the crystal structure reported for $[Fe_2S_2(S\text{-}p\text{-}MeC_6H_4)_4]^{2-}$,[18] while large angles (89 and 86°) between them were observed in the crystal structure of **5b**. A similar angle due to steric congestion has been observed for the crystal structure of $[Fe_2S_2(tmbt)_4]^{2-}$.[31]

The Fe···Fe distance (2.671(6) Å) of **5b** is definitely shortened by approximately 0.02 Å compared to the distance of 2.691 Å in $[Fe_2S_2(S\text{-}p\text{-}MeC_6H_4)_4]^{2-}$ reported by Mayerle et al.[18] A core distortion as evaluated by the dihedral angle of Fe(1)−S(3)−Fe(1)*−S(3)* = −4.2° from a symmetrical $(Fe_2S_2)^{2+}$ core (0°) was found for **5b**. Typical examples for the symmetrical core having Fe···Fe distances of 2.698(1) and 2.698(5) Å were reported for $[Fe_2S_2(S_2\text{-}o\text{-}xyl)_2]^{2-}$ [18] and $[Fe_2S_2(tmbt)_4]^{2-}$,[31] respectively. At present, no report on such a distorted $(Fe_2S_2)^{2+}$ core has been found previously for the plant-type ferredoxin [2Fe-2S] model complexes.

The Fe−S−C angles of **5b** are 107.1(9) and 109.1(8)° similar to those in $[Fe_2S_2(S\text{-}p\text{-}MeC_6H_4)_4]^{2-}$ rather than to those in $[Fe_2S_2(S_2\text{-}o\text{-}xyl)_2]^{2-}$.[18] The ordinary Fe−S−C angle (106−112°) in $[M(SC_6H_5)_4]^{2-}$ (M = Zn(II), Cd(II), Co(II), Ni(II), Mn(II)) has been interpreted as due to the covalent nature of the M−S bond.[32,33]

**Detection of the NH···S Hydrogen Bond by IR Spectroscopy.** Figure 3a,b shows the selected IR spectra of $(NEt_4)_2[Fe_4S_4(S\text{-}2\text{-}t\text{-}BuCONHC_6H_4\}_4]$ (**2a**) in the solid state compared with the disulfides. The single NH···S hydrogen-bonded complex exhibits an NH band at 3314 $cm^{-1}$ and a CO band at 1670 $cm^{-1}$ in the solid state. Bis(2-(pivaloylamino)phenyl) disulfide possesses two distinct NH bands at 3389 and 3251

**Table 2.** Selected Bond Lengths and Bond Angles in $(PPh_4)_2[Fe_4S_4\{S\text{-}2,6\text{-}(CH_3CONH)_2C_6H_3\}_4]$ (**1b**)

| | | | |
|---|---|---|---|
| Distances (Å) | | | |
| Fe1−S1 | 2.278(2) | S1−C11 | 1.778(6) |
| Fe2−S2 | 2.268(2) | S2−C21 | 1.773(6) |
| Fe3−S3 | 2.290(2) | S3−C31 | 1.780(6) |
| Fe4−S4 | 2.271(2) | S4−C41 | 1.764(7) |
| mean | 2.277 | mean | 1.774 |
| Fe1−S6 | 2.275(2) | Fe3−S5 | 2.293(2) |
| Fe1−S7 | 2.285(2) | Fe3−S6 | 2.268(2) |
| Fe1−S8 | 2.268(2) | Fe3−S8 | 2.286(2) |
| Fe2−S5 | 2.273(2) | Fe4−S5 | 2.262(2) |
| Fe2−S7 | 2.264(2) | Fe4−S6 | 2.284(2) |
| Fe2−S8 | 2.286(2) | Fe4−S7 | 2.283(2) |
| | | mean | 2.277 |
| Fe1···Fe2 | 2.727(1) | S5−S6 | 3.592(2) |
| Fe1···Fe3 | 2.748(1) | S5−S7 | 3.593(2) |
| Fe1···Fe4 | 2.720(1) | S5−S8 | 3.616(2) |
| Fe2···Fe3 | 2.731(1) | S6−S7 | 3.617(2) |
| Fe2···Fe4 | 2.702(1) | S6−S8 | 3.570(2) |
| Fe3···Fe4 | 2.730(1) | S7−S8 | 3.589(2) |
| mean | 2.726 | mean | 3.596 |
| Angles and Torsion Angles (deg) | | | |
| Fe1−S1−C11 | 103.1(2) | Fe1−S1−C11−C12 | 85.9(5) |
| Fe2−S2−C21 | 104.9(2) | Fe2−S2−C21−C22 | 85.1(5) |
| Fe3−S3−C31 | 98.0(2) | Fe3−S3−C31−C32 | 85.7(5) |
| Fe4−S4−C41 | 102.5(2) | Fe4−S4−C41−C42 | 87.3(5) |
| mean | 102.1 | mean | 86.0 |

**Table 3.** Selected Bond Distances and Angles in $(NEt_4)_2[Fe_2S_2\{S\text{-}2,6\text{-}(t\text{-}BuCONH)_2C_6H_3\}_4]$ (**5b**)

| | | | |
|---|---|---|---|
| Distances (Å) | | | |
| Fe1−S1 | 2.308(8) | Fe1−S2 | 2.328(7) |
| Fe1−S3 | 2.198(7) | Fe1−S3* | 2.203(6) |
| S1−C11 | 1.78(2) | S2−C21 | 1.77(2) |
| Fe1···Fe1* | 2.671(6) | S1···S2 | 3.74(1) |
| S3···S3* | 3.47(1) | | |
| Angles (deg) | | | |
| Fe1−S1−C11 | 107.1(9) | Fe1−S2−C21 | 109.1(8) |
| S1−Fe1−S3 | 110.3(3) | S2−Fe1−S3 | 112.7(3) |
| S1−Fe1−S2 | 107.7(3) | S3−Fe1−S3* | 104.1(2) |
| Torsion Angles (deg) | | | |
| S3−Fe1−S1−C11 | −165.8 | S3−Fe1−S2−C21 | −75.1(9) |
| Fe1−S1−C11−C12 | 89(2) | Fe1−S2−C21−C22 | 86(1) |
| Fe1−S3−Fe1*−S3* | 11.8(4) | S1−Fe1−Fe1*−S1* | −4.2(4) |

(31) Ueyama, N.; Ueno, S.; Sugawara, T.; Tatsumi, K.; Nakamura, A.; Yasuoka, N. *J. Chem. Soc., Dalton Trans.* **1991**, 2723.

(32) Swenson, D.; Baenzinger, N. C.; Coucouvanis, D. *J. Am. Chem. Soc.* **1978**, *100*, 1933.

(33) Ueyama, N.; Sugawara, T.; Sasaki, K.; Nakamura, A.; Yamazaki, S.; Wakatsuki, Y.; Yamazaki, H.; Yasuoka, N. *Inorg. Chem.* **1988**, *27*, 741.

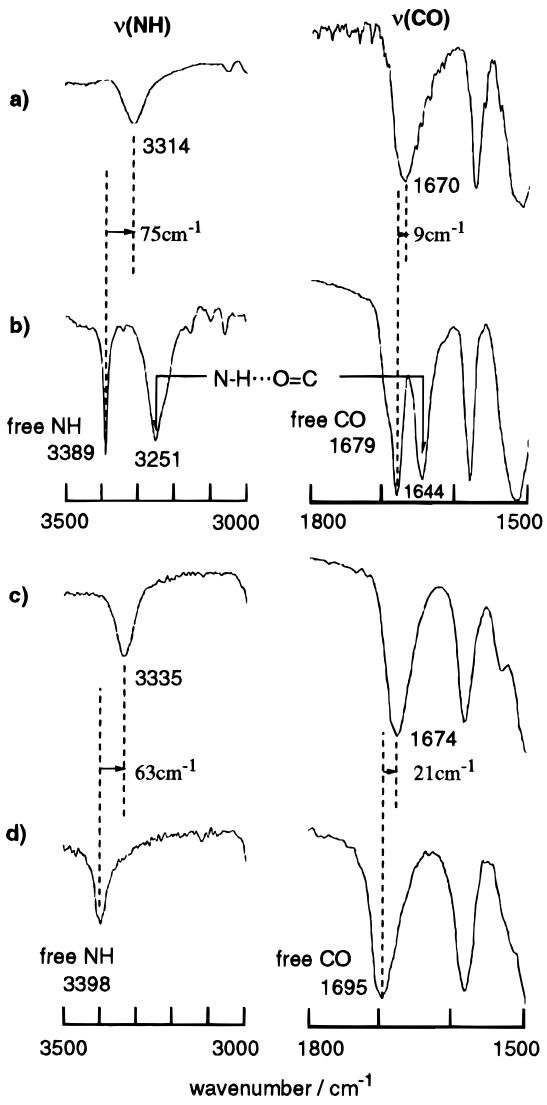


**Figure 3.** Selected IR bands of (a) $(NEt_4)_2[Fe_4S_4(S\text{-}2\text{-}t\text{-}BuCONHC_6H_4)_4]$ (**2a**), (b) bis(2-*t*-$BuCONHC_6H_4$} disulfide, (c) $(NEt_4)_2[Fe_4S_4\{S\text{-}2,6\text{-}(t\text{-}BuCONH)_2C_6H_3\}_4]$ (**2b**), and (d) bis{2,6-(*t*-$BuCONH)_2C_6H_3$} disulfide in the solid state.

$cm^{-1}$ assignable to noninteracted free NH stretching and intermolecularly hydrogen-bonded NH stretching, respectively, as reported previously.[34] The corresponding CO bands are observed at 1679 and 1644 $cm^{-1}$, which are similarly assignable to the free CO and the intermolecularly hydrogen-bonded CO stretching, respectively. The short wavenumber shift of the amide NH in the NH···S hydrogen bond is 75 $cm^{-1}$ from 3389 $cm^{-1}$ of free NH stretching, whereas the CO shift is only 9 $cm^{-1}$. The wavenumbers of various model complexes are listed in Table 4. Similar shifts have been observed for various single NH···S hydrogen-bonded metal complexes, e.g., 59 $cm^{-1}$ for $[Mo^{V}O(S\text{-}2\text{-}t\text{-}BuCONHC_6H_4)_4]^-$ and 163 $cm^{-1}$ for $[Cu^{I}(S\text{-}2\text{-}t\text{-}BuCONHC_6H_4)_3]^{2-}$.[35,36]

Figure 3c,d also shows the amide NH and CO regions of the IR spectra of $(NEt_4)_2[Fe_4S_4\{S\text{-}2,6\text{-}(t\text{-}BuCONH)_2C_6H_3\}_4]$ (**2b**) and the corresponding disulfide in the solid state. The doubly NH···S hydrogen-bonded complex exhibits an NH band at 3335 $cm^{-1}$ and a CO band at 1674 $cm^{-1}$. On the basis of the NH stretching (3398 $cm^{-1}$) and CO stretching (1695 $cm^{-1}$) for the disulfide, (S-2-*t*-$BuCONHC_6H_4)_2$, the estimated shift for the NH···S hydrogen-bonded NH stretching is 63 $cm^{-1}$ and that for the free CO stretching is 21 $cm^{-1}$. $(NEt_4)_2[Fe_4S_4(S\text{-}2\text{-}CF_3\text{-}CONHC_6H_4)_4]$ (**3a**) shows an NH band at 3257 $cm^{-1}$ and a CO band at 1721 $cm^{-1}$ in the solid state. Since the corresponding disulfide has intermolecular NH···O hydrogen bond, it is difficult to evaluate the IR shift for the NH···S hydrogen bonding.

**Table 4.** IR Shifts of Amide $\Delta\nu$(NH) and $\Delta\nu$(CO) in $[Fe_4S_4(S\text{-}2\text{-}RCONHC_6H_4)_4]^{2-}$ (R = $CH_3$, *t*-Bu, $CF_3$) and $[Fe_4S_4\{S\text{-}2,6\text{-}(RCONH)_2C_6H_4\}_4]^{2-}$ in the Solid State

| complexes | $\nu$(NH) ($\Delta\nu$(NH))[a] ($cm^{-1}$) | $\nu$(CO) ($\Delta\nu$(CO))[a] ($cm^{-1}$) |
|---|---|---|
| $(NEt_4)_2[Fe_4S_4(S\text{-}2\text{-}t\text{-}BuCONHC_6H_4)_4]$ (**2a**) | 3315 (74) | 1671 (8) |
| $(NEt_4)_2[Fe_4S_4(S\text{-}2\text{-}CF_3CONHC_6H_4)_4]$ (**3a**) | 3257 | 1721 |
| $(NEt_4)_2[Fe_4S_4\{S\text{-}2,6\text{-}(t\text{-}BuCONH)_2C_6H_3\}_4]$ (**2b**) | 3335 (63) | 1674 (21) |
| $(NMe_4)_2[Fe_4S_4\{S\text{-}2,6\text{-}(CF_3CONH)_2C_6H_3\}_4]$ (**3b**) | 3286 | 1724 |
| $(NEt_4)_2[Fe_2S_2(S\text{-}2\text{-}t\text{-}BuCONHC_6H_4)_4]$ (**5a**) | 3321 (68) | 1674 (5) |
| $(NEt_4)_2[Fe_2S_2\{S\text{-}2,6\text{-}(t\text{-}BuCONH)_2C_6H_3\}_4]$ (**5b**) | 3332 (66) | 1675 (20) |

[a] $\Delta\nu$(NH) or $\Delta\nu$(CO) was obtained from the difference in amide $\nu$(NH) or $\nu$(CO) between the model complex and corresponding disulfide.

In addtion, similar NH bands were observed at 3339 $cm^{-1}$ at 10 mM concentration for a dichloromethane solution of **2b** and the CO band appears at 1672 $cm^{-1}$. No concentration dependence was observed for the dichloromethane solutions. Since these data are almost the same as those of **2b** in the solid state, the complex has intramolecular hydrogen bonds in solution as in the solid state. This similarity in both solid and solution structures is due to the steric congestion around amide groups in the o,o′-(diacylamino)benzenethiolate.

On the other hand, the other doubly NH···S hydrogen-bonded complex, $(NMe_4)_2[Fe_4S_4\{S\text{-}2,6\text{-}(CF_3CONH)_2C_6H_3\}_4]$ (**3b**), shows intricate IR bands, accompanied by strengthening of the NH···S hydrogen bonds by the electron-withdrawing trifluoromethyl group. The complex **3b** exhibits an NH band at 3286 $cm^{-1}$ and a broad CO band at 1724 $cm^{-1}$. On the contrary, the corresponding disulfide, $\{S\text{-}2,6\text{-}(CF_3CONH)_2C_6H_3\}_2$, gives two separate NH bands at 3363 and 3334 $cm^{-1}$ and three CO bands at 1741, 1729, and 1717 $cm^{-1}$. The shifts of the NH and CO bands from each standard stretching of the disulfide are 77 and 17 $cm^{-1}$, respectively, when the NH···S hydrogen bond forms. The formation of the hydrogen bond is further supported by the X-ray analysis of **3b** because the two amide NH groups are directed to the sulfur atom in the crystal structure.

Figure 4a shows the IR spectra of $(NEt_4)_2[Fe_2S_2(S\text{-}2\text{-}t\text{-}BuCONHC_6H_4)_4]$ (**5a**) and of the corresponding disulfide, (S-2-*t*-$BuCONHC_6H_4)_2$, in the solid states. The complex exhibits only one amide NH stretching at 3321 $cm^{-1}$. When the band at 3389 $cm^{-1}$ is adopted as a standard for the free NH stretching, the shift of the amide NH for **5a** amounts to 68 $cm^{-1}$. On the other hand, since the amide CO stretchings for the disulfide are observed at 1679 and 1644 $cm^{-1}$, and the amide CO band for the thiolate complex is found at 1674 $cm^{-1}$, the $\nu$(CO) shift by the NH···S hydrogen bond is only 5 $cm^{-1}$. If the NH and CO groups are involved in the NH···O═C hydrogen bond, the shift should be large and close to 35 $cm^{-1}$ for the disulfide. The small CO shift (5 $cm^{-1}$) is due to an electronic perturbation on the same amide group accompanied by the formation of the NH···S hydrogen bond. Thus, the existence of the intramolecular NH···S hydrogen bond was also clearly shown for **5a**.

Figure 4b shows the selected IR spectra of $(NEt_4)_2[Fe_2S_2\{S\text{-}2,6\text{-}(t\text{-}BuCONH)_2C_6H_3\}_4]$ (**5b**) and the corresponding disulfide, $\{S\text{-}2,6\text{-}(t\text{-}BuCONH)_2C_6H_3\}_2$, on a KBr disk. The complex

(34) Ueyama, N.; Okamura, T.; Yamada, Y.; Nakamura, A. *J. Org. Chem.* **1995**, *60*, 4893.
(35) Ueyama, N.; Okamura, T.; Nakamura, A. *J. Am. Chem. Soc.* **1992**, *114*, 8129.
(36) Okamura, T.; Ueyama, N.; Nakamura, A.; Ainscough, E. W.; Brodie, A. M.; Waters, J. M. *J. Chem. Soc., Chem. Commun.* **1993**, 1658.

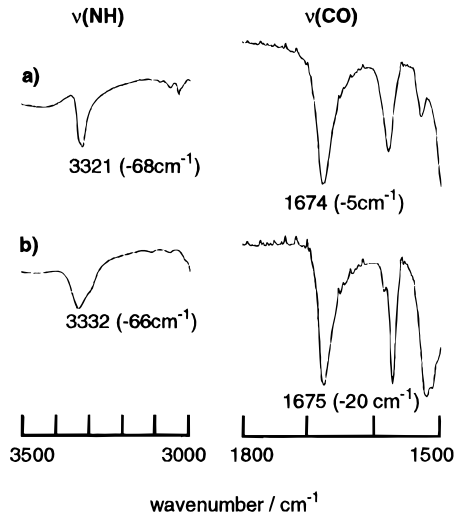


**Figure 4.** Selected IR bands in the amide regions of (a) $(NEt_4)_2[Fe_2S_2(S\text{-}2\text{-}t\text{-}BuCONHC_6H_4)_4]$ and (b) $(NEt_4)_2[Fe_2S_2\{S\text{-}2,6\text{-}(t\text{-}BuCONH)_2C_6H_3\}_4]$ in the solid states. The shifts were estimated from the corresponding disulfide IR bands.

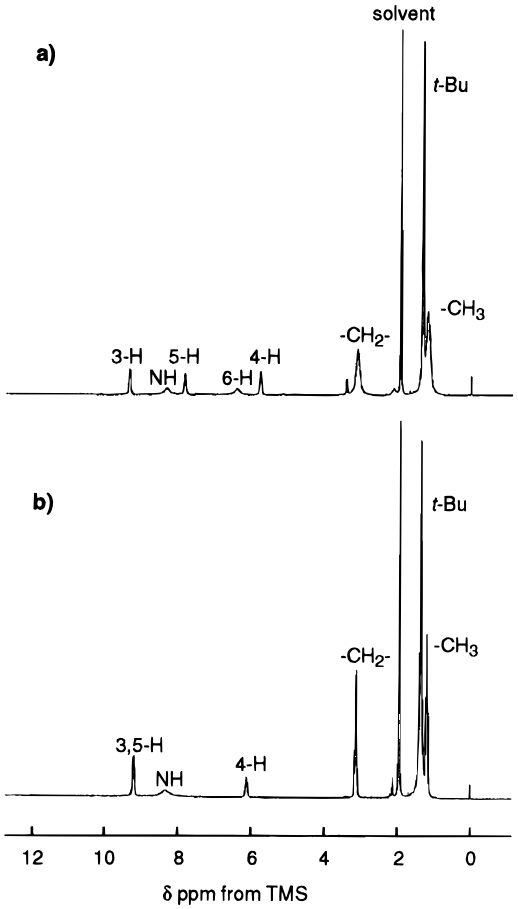


**Figure 5.** $^1$H NMR spectra of (a) $(NEt_4)_2[Fe_4S_4(S\text{-}2\text{-}t\text{-}BuCONHC_6H_4)_4]$ (**2a**) and (b) $(NEt_4)_2[Fe_4S_4\{S\text{-}2,6\text{-}(t\text{-}BuCONH)_2C_6H_3\}_4]$ (**2b**) in acetonitrile-$d_3$ at 30 °C.

shows a sharp NH band at 3332 cm$^{-1}$ with a shift of 66 cm$^{-1}$ from that of the disulfide, whereas the CO band is observed at 1675 cm$^{-1}$ with a shift of 20 cm$^{-1}$ from that of the disulfide. Similar NH and CO bands were observed at 3329 and 1668 cm$^{-1}$, respectively, for a dichloromethane solution (10 mM concentration) of **5b**.

**$^1$H NMR Spectra.** Figure 5 shows the $^1$H NMR spectra of ferredoxin model complexes having singly and doubly NH···S hydrogen-bonded ligands, $(NEt_4)_2[Fe_4S_4(S\text{-}2\text{-}t\text{-}BuCONHC_6H_4)_4]$ (**2a**) and $(NEt_4)_2[Fe_4S_4\{S\text{-}2,6\text{-}(t\text{-}BuCONH)_2C_6H_3\}_4]$ (**2b**), in acetonitrile-$d_3$. The singly NH···S hydrogen-bonded complex, **2a**, exhibits peaks assignable to 3-, 4-, 5-, and 6-H at 9.37, 6.44, 5.79, and 7.86 ppm, respectively. A broad NH signal is observed at 8.35 ppm, which was assigned using a $CH_3OD$ addition method. The NH signal is slightly isotropically contact-shifted compared with the NH signal at 8.34 ppm of bis(2-(pivaloylamino)phenyl) disulfide in acetonitrile-$d_3$, e.g., $(\Delta H/H_0)^{iso} = +0.17$ for $(NEt_4)_2[Fe_4S_4(S\text{-}2\text{-}CH_3CONHC_6H_4)_4]$ (**1a**) and $(\Delta H/H_0)^{iso} = +0.01$ for **2a**. The isotropic shift of the NH···S hydrogen-bonded NH signal in various peptide model complexes is also small as reported for $[Fe_4S_4(Z\text{-}\mathbf{cys}\text{-}Gly\text{-}NHC_6H_4\text{-}p\text{-}X)_4]^{2-}$ (X = OMe, H, Cl, CN; Z = (benzyloxy)-carbonyl) in acetonitrile-$d_3$ at room temperature.[7] A similar observation of amide NH signals probably associated with NH···S hydrogen bonding has been reported for an aqueous solution of oxidized *Clostridium acidi-urici* ferredoxin.[37]

In the case of the doubly NH···S hydrogen-bonded complex, $(PPh_4)_2[Fe_4S_4\{S\text{-}2,6\text{-}(t\text{-}BuCONH)_2C_6H_3\}_4]$, slight isotropic-shifted signals are found at 8.32 ppm for amide NH, 9.20 ppm for *m*-phenyl H,, and 6.12 ppm for *p*-phenyl H in acetonitrile-$d_3$.

Table 5 summarizes the isotropic contact shift of each signal of these complexes. The isotropic shift of the proton signals except for the amide NH is substantially similar to those of ferredoxin model complexes with *p*-substituted benzenethiolate complexes which have been studied in detail.[38] It is likely that the difference in the isotropic shift of the NH signals between the single and double NH···S hydrogen-bonded complexes is ascribed to the structure around S−C(Ph) with the conjugation between S $p\pi$ and phenyl $p\pi$.

The slightly contact-shifted signals of the 2-(pivaloylamino)-benzenethiolate ligand in $(NEt_4)_2[Fe_2S_2(S\text{-}2\text{-}t\text{-}BuCONHC_6H_4)_4]$ (**5a**) in acetonitrile-$d_3$ at 303 K are observed at 10.9 ppm for 3-ArH, 8.9 ppm for 5-ArH, 4.6 ppm (broad) for 6-ArH, 3.1 ppm for 4-ArH, and 6.8 ppm (broad) for amide NH. The amide NH signal was assigned by disappearance of the signal on deuteration. The large shift of 6-ArH is due to an anisotropic shielding effect by the CO group in the vicinity. Tentatively, the isotropic shifts of these signals were calculated in order to compare them with the values for $[Fe_2S_2(SC_6H_5)_4]^{2-}$ reported by Hagen et al.[39] and are listed in Table 5. These isotropic shifts are similar to those of the reported model complexes.[38,39] When the unpaired spin density is distributed to the conjugated S p$\pi$, aromatic p$\pi$, and amide p$\pi$ orbitals, the amide NH signal would appear with a plus isotropic shift. The minus shift is ascribed to a direct bond formation between the amide NH and the sulfur atom, and the sign is governed by the sign of the spin at the sulfur atom. Thus, the minus isotropic shift of the amide NH indicates the formation of the NH···S hydrogen bond in these [2Fe-2S] complexes.

In the case of the doubly NH···S hydrogen-bonded complexes, the isotropic shifts are essentially similar to those of the singly NH···S hydrogen-bonded complexes as listed in Table 5 except for the NH signal. Here, the isotropic shift for amide NH is small. It is likely that double hydrogen bonds decrease each shift and become almost the same as the conjugated through-bonding effect having a different spin sign.

**Electronic Absorption Spectra.** Absorption maxima in the UV−visible spectra of $(NEt_4)_2[Fe_4S_4(S\text{-}2\text{-}RCONHC_6H_4)_4]$ (R

(37) Packer, E. L.; Sweeney, W. V.; Thompson, K. F.; Sternlicht, H.; Shaw, E. N. *J. Biol. Chem.* **1877**, *252*, 2245.
(38) Holm, R. H.; Phillips, W. D.; Averill, B. A.; Mayerle, J. J. *J. Am. Chem. Soc.* **1974**, *96*, 2109.
(39) Hagen, K. S.; Reynolds, J. G.; Holm, R. H. *J. Am. Chem. Soc.* **1981**, *103*, 4054.

**Table 5.** Isotropic Shift Value (ppm) of $[Fe_4S_4\{S\text{-}2\text{-}(RCONH)C_6H_4\}_4]^{2-}$ (R = $CH_3$, *t*-Bu, $CF_3$), $[Fe_4S_4\{S\text{-}2,6\text{-}(RCONH)_2C_6H_3\}_4]^{2-}$, $(NEt_4)_2[Fe_2S_2(S\text{-}2\text{-}RCONHC_6H_4)_4]$, and $(NEt_4)_2[Fe_2S_2\{S\text{-}2,6\text{-}(RCONH)_2C_6H_3\}_4]$ in Acetonitrile-$d_3$ at 303 K

| | Ar-3H | Ar-4H | Ar-5H | Ar-6H | NH |
|---|---|---|---|---|---|
| $(NEt_4)_2[Fe_4S_4(S\text{-}2\text{-}RCONHC_6H_4)_4]$ (**1a**) | +1.33 | −1.54 | +0.74 | −0.96 | +0.17 |
| $(NEt_4)_2[Fe_4S_4(S\text{-}2\text{-}t\text{-}BuCONHC_6H_4)_4]$ (**2a**) | +1.27 | −1.64 | +0.76 | −1.03 | +0.01 |
| $(NEt_4)_2[Fe_4S_4(S\text{-}2\text{-}CF_3CONHC_6H_4)_4]$ (**3a**) | +1.49 | −1.58 | +0.64 | −1.12 | ∼+0.1 |
| $(NEt_4)_2[Fe_4S_4\{S\text{-}2,6\text{-}(CH_3CONH)_2C_6H_3\}_4]$ (**1b**) | +1.23 | −1.26 | +1.23 | | +0.09 |
| $(NEt_4)_2[Fe_4S_4\{S\text{-}2,6\text{-}(t\text{-}BuCONH)_2C_6H_3\}_4]$ (**2b**) | +1.23 | −1.30 | +1.23 | | −0.03 |
| $(NEt_4)_2[Fe_4S_4\{S\text{-}2,6\text{-}(CF_3CONH)_2C_6H_3\}_4]$ (**3b**) | +1.21 | −1.26 | +1.21 | | +0.28 |
| $(NEt_4)_2[Fe_2S_2(S\text{-}2\text{-}RCONHC_6H_4)_4]$ (**4a**) | +2.8 | −4.1 | +2.0 | −2.7 | −1.0 |
| $(NEt_4)_2[Fe_2S_2(S\text{-}2\text{-}t\text{-}BuCONHC_6H_4)_4]$ (**5a**) | +2.9 | −4.0 | +1.8 | −2.7 | −1.4 |
| $(NEt_4)_2[Fe_2S_2(S\text{-}2\text{-}CF_3CONHC_6H_4)_4]$ (**6a**) | +3.1 | −3.9 | +1.7 | −2.9 | −1.1 |
| $(NEt_4)_2[Fe_2S_2\{S\text{-}2,6\text{-}(CH_3CONH)_2C_6H_3\}_4]$ (**4b**) | +2.8 | −4.7 | +2.8 | | +0.5 |
| $(NEt_4)_2[Fe_2S_2\{S\text{-}2,6\text{-}(t\text{-}BuCONH)_2C_6H_3\}_4]$ (**5b**) | +2.5 | −4.4 | +2.5 | | −0.2 |
| $(NEt_4)_2[Fe_2S_2\{S\text{-}2,6\text{-}(CF_3CONH)_2C_6H_3\}_4]$ (**6b**) | +2.7 | −4.4 | +2.7 | | +0.1 |

**Table 6.** Absorption Maxima of $[Fe_4S_4\{S\text{-}o\text{-}(RCONH)C_6H_4\}_4]$ and $[Fe_4S_4\{S\text{-}o,o'\text{-}(RCONH)_2C_6H_3\}_4]$ in Acetonitrile at 300 K

| | $\lambda_{max}$/nm ($\epsilon$/$M^{-1}$ $cm^{-1}$) | | | |
|---|---|---|---|---|
| **1a** | 322 (sh, 19 000) | 445 (sh, 14 000) | | |
| **2a** | 315 (sh, 21 000) | 423 (sh, 15 000) | | |
| **3a** | 359 (sh, 22 000) | 412 (sh, 18 000) | | |
| **1b** | | 369 (23 000) | 423 (sh, 20 000) | |
| **2b** | 347 (sh, 25 000) | 369 (25 000) | 421 (sh, 22 000) | |
| **3b** | | 363 (27 000) | 418 (sh, 19 200) | |
| **4a** | 341 (16 900) | 426 (16 100) | 469 (sh, 12 500) | |
| **5a** | 341 (16 800) | 422 (14 700) | | 513 (sh, 9500) |
| **6a** | | 417 (12 400) | 463 (sh, 9700) | 512 (sh, 7500) |
| **4b** | 337 (18 400) | 430 (12 500) | | |
| **5b** | 346 (15 800) | 432 (21 200) | | 520 (sh, 7700) |
| **6b** | 358 (13 300) | 409 (sh, 8200) | | 528 (3800) |
| | | | | 600 (sh, 2600) |

= $CH_3$ (**1a**), *t*-Bu (**2a**), $CF_3$ (**3a**)) in acetonitrile at room temperature are listed in Table 6. All the model complexes having single NH···S hydrogen-bonded thiolate exhibit maxima at ca. 320−360 nm (sh, 19 000−22 000) and 412−445 nm (sh, 14 000−18 000). A slightly different shape around 440 nm from that of $(NEt_4)_2[Fe_4S_4(SPh)_4]$ was observed for the single NH···S hydrogen-bonded model complexes. Arenethiolate model complexes, e.g. $(NEt_4)_2[Fe_4S_4(SC_6H_4\text{-}p\text{-}X)_4]$ (X = $CH_3$, H, $NO_2$), show a characteristic maximum at ca. 450 nm with a red-shift by the electron-withdrawing *p*-$NO_2$ substituent. When comparison was made among absorption maxima at ca. 450 nm for the three complexes **1a**, **2a**, and **3a**, a slight red-shift was observed due to strengthening of the NH···S hydrogen bonding at the *o*-positions.

Various ferredoxin model complexes, $[Fe_4S_4(SR)_4]^{2-}$, having alkane- and arenethiolate ligands, $(NEt_4)_2[Fe_4S_4\{S\text{-}2,6\text{-}(RCONH)_2C_6H_3\}_4]$ (R = $CH_3$ (**1b**), *t*-Bu (**2b**), $CF_3$ (**3b**)), have been studied in terms of the detailed characteristic absorption maxima.[10,40] Alkanethiolate complexes, e.g., $(NEt_4)_2[Fe_4S_4(SCH_2C_6H_5)_4]$,[3] exhibit strong maxima at 286 nm (sh, 28 800) and 420 nm (18 500) in DMF at room temperature, whereas native cysteine-containing ferredoxins in an aqueous solution have been reported to exhibit a slightly blue-shifted absorption maximum, e.g., 390 nm for *Bacillus stearothermophilus* ferredoxin[41] and 390 nm for *Bacillus thermoproteolyticus* ferredoxin.[42] The double NH···S hydrogen-bonded complexes show characteristic absorption maxima at 363 nm (27 000) and 418 nm (19 200) for **3b**. The absorption maxima in this region have been theoretically proposed to be due to essentially S → Fe charge transfer bands.[43]

Although two characteristic absorption maxima at 338 and 490 nm in DMF have been reported for $(NEt_4)_2[Fe_2S_2(SC_6H_5)_4]$, 2-(acylamino)benzenethiolate complexes exhibit absorption maxima or shoulders at ca. 300, ca. 340, ca. 430, and 470 nm in DMF or in acetonitrile. These maxima are similar in value to those of simple alkanethiolate complexes, e.g., $[Fe_2S_2(S_2\text{-}o\text{-}xyl)_2]^{2-}$ ($S_2$-*o*-xyl = *o*-xylene-α,α′-dithiolate),[18] cysteine-containing peptide complexes, e.g., $[Fe_2S_2(Z\text{-}\mathbf{cys}\text{-}Ala\text{-}Ala\text{-}\mathbf{cys}\text{-}OMe)_2]^{2-}$ (Z = benzyloxycarbonyl),[20] and native plant-type ferredoxins.[44]

On the other hand, 2,6-bis(acylamino)benzenethiolate [2Fe-2S] complexes, $(NEt_4)_2[Fe_2S_2\{S\text{-}2,6\text{-}(CR_3CONH)_2C_6H_3\}_4]$ (R = $CH_3$ (**4b**), *t*-Bu (**5b**), $CF_3$ (**6b**)), in acetonitrile exhibit absorption maxima at 300, 340, 430, 530, and 600 nm which are also similar to those of native plant-type ferredoxins.[44] The complexes **6b** and **5b** having double NH···S hydrogen bonds give different absorption maxima in acetonitrile from those of the singly NH···S hydrogen-bonded model complexes. **6b** exhibits bands at 358 and 409 nm (sh, 8200 $M^{-1}$ $cm^{-1}$), whereas **5b** shows strong bands at 364 and 432 nm (21 200 $M^{-1}$ $cm^{-1}$). Thus, the large change in absorption maxima in a [2Fe-2S] ferredoxin model complex occurs by the introduction of two amide groups at the *o*,*o*′-positions. The spectrum in the LMCT region indicates an extensive change in the electronic state of the $[Fe_2S_2(SR)_4]^{2-}$ cluster which presumably comes from the distortion of $[Fe_2S_2]^{2+}$ core as determined by the X-ray crystallographic analysis of **5b**.

**Electrochemical Properties of [4Fe-4S] and [2Fe-2S] Model Complexes.** Single NH···S hydrogen-bonded model complexes exhibit the quasi-reversible redox couple and the peak separation of $[Fe_4S_4(SR)_4]^{3-}/[Fe_4S_4(SR)_4]^{2-}$ in acetonitrile at room temperature as listed in Table 7. On the basis of a comparison in the redox potentials between $[Fe_4S_4(S\text{-}2\text{-}t\text{-}BuCONHC_6H_4)_4]^{2-}$ (**2a**) and $[Fe_4S_4(SPh)_4]^{2-}$,[45] one NH···S hydrogen bond can positively shift in 0.09 V similar to the range of 0.07−0.08 V estimated from the number of NH···S hydrogen bonds found by the X-ray crystallographic analysis[1,46] of *P. aerogenes* ferredoxin.[18] The single NH···S hydrogen bond of $(NEt_4)_2[Fe_4S_4(S\text{-}2\text{-}CF_3CONHC_6H_4)_4]$ (**3a**) contributes to the shift by 0.2 V due to the strengthening of the hydrogen bond by the electron-withdrawing effect of $CF_3$.

Doubly NH···S hydrogen-bonded model complexes have relatively large positive-shifted redox potentials of the 3−/2− couple at −0.62 V vs SCE for $(NMe_4)_2[Fe_4S_4\{S\text{-}2,6\text{-}(CF_3CONH)_2C_6H_3\}_4]$ (**3b**), −0.72 V vs SCE for $(PPh_4)_2[Fe_4S_4\{S\text{-}$

(40) Nakamura, A.; Ueyama, N. *Encyclopedia of Inorganic Chemistry*; John Wiley & Sons Ltd.: Chichester, New York, Brisbane, Toronto, Singapore, 1994; Vol. 4, p 1883.
(41) Mullinger, R. N.; Cammack, R.; Rao, K. K.; Hall, D. O.; Dickson, D. P. E.; Johnson, C. E.; Rush, J. D.; Simopoulus, A. *Biochem. J.* **1975**, *151*, 75.
(42) Yang, S.; Ljungdahl, L. G.; LeGall, J. *J. Bacterial.* **1977**, *130*, 7487.
(43) Aizman, A.; Case, D. A. *J. Am. Chem. Soc.* **1982**, *104*, 3269.
(44) Stephens, P. J.; Thomson, A. J.; Dunn, J. B. R.; Keiderling, T. A.; Rawling, J.; Rao, K. K.; Hall, D. O. *Biochemistry* **1978**, *17*, 4770.
(45) Cambray, J.; Lane, R. W.; Wedd, A. G.; Johnson, R. W.; Holm, R. H. *Inorg. Chem.* **1977**, *16*, 2565.
(46) Adman, E.; Watenpaugh, K. D.; Jensen, L. H. *Proc. Natl. Acad. Sci. U.S.A.* **1975**, *72*, 4854.

**Table 7.** Electrochemical Data for $[Fe_4S_4\{S\text{-}2\text{-}(RCONH)C_6H_4\}_4]^{2-}$ (R = $CH_3$, *t*-Bu, $CF_3$), $[Fe_4S_4\{S\text{-}2,6\text{-}(RCONH)_2C_6H_3\}_4]^{2-}$, $(NEt_4)_2[Fe_2S_2(S\text{-}2\text{-}RCONHC_6H_4)_4]$, and $(NEt_4)_2[Fe_2S_2\{S\text{-}2,6\text{-}(RCONH)_2C_6H_3\}_4]$ in Acetonitrile at Room Temperature

| | $E_{1/2}$, V vs SCE | $E_{pa} - E_{pc}$, V | $i_{pa}/i_{pc}$ |
|---|---|---|---|
| $(NEt_4)_2[Fe_4S_4(S\text{-}2\text{-}CH_3CONHC_6H_4)_4]$ (**1a**) | −0.83 | 0.18 | 1.0 |
| $(NEt_4)_2[Fe_4S_4(S\text{-}2\text{-}t\text{-}BuCONHC_6H_4)_4]$ (**2a**) | −0.90 | 0.11 | 1.0 |
| $(NEt_4)_2[Fe_4S_4(S\text{-}2\text{-}CF_3CONHC_6H_4)_4]$ (**3a**) | −0.78 | 0.21 | 0.9 |
| $(PPh_4)_2[Fe_4S_4\{S\text{-}2,6\text{-}(CH_3CONH)_2C_6H_3\}_4]$ (**1b**) | −0.72 | 0.20 | 0.7 |
| $(NEt_4)_2[Fe_4S_4\{S\text{-}2,6\text{-}(t\text{-}BuCONH)_2C_6H_3\}_4]$ (**2b**) | −0.80 | 0.12 | 1.0 |
| $(NMe_4)_2[Fe_4S_4\{S\text{-}2,6\text{-}(CF_3CONH)_2C_6H_3\}_4]$ (**3b**) | −0.62 | 0.16 | 0.6 |
| $(NEt_4)_2[Fe_2S_2(S\text{-}2\text{-}CH_3CONHC_6H_4)_4]$ (**4a**) | −0.90 | 0.14 | 0.5 |
| $(NEt_4)_2[Fe_2S_2(S\text{-}2\text{-}t\text{-}BuCONHC_6H_4)_4]$ (**5a**) | −0.94 | 0.27 | 0.5 |
| $(NEt_4)_2[Fe_2S_2(S\text{-}2\text{-}CF_3CONHC_6H_4)_4]$ (**6a**) | −0.80 | 0.21 | 0.5 |
| $(NEt_4)_2[Fe_2S_2\{S\text{-}2,6\text{-}(CH_3CONH)_2C_6H_3\}_4]$ (**4b**) | −0.64 | 0.21 | 0.3 |
| $(NEt_4)_2[Fe_2S_2\{S\text{-}2,6\text{-}(t\text{-}BuCONH)_2C_6H_3\}_4]$ (**5b**) | −0.79 | 0.22 | 0.2 |
| $(NEt_4)_2[Fe_2S_2\{S\text{-}2,6\text{-}(CF_3CONH)_2C_6H_3\}_4]$ (**6b**) | −0.59 | 0.13 | 0.2 |

2,6-$(CH_3CONH)_2C_6H_3\}_4]$ (**1b**), and −0.80 V vs SCE for $(NEt_4)_2[Fe_4S_4\{S\text{-}2,6\text{-}(t\text{-}BuCONH)_2C_6H_3\}_4]$ (**2b**) in acetonitrile. The strengthening of two NH···S hydrogen bonds with an electron-withdrawing group, $CF_3$, results in the further positive shift of the redox potential.

Interestingly, the redox couple of 2−/1− is also shifted to a similar extent accompanied by the positive shift of the 3−/2− redox couple. The redox couple of 2−/1− could not be observed in the range of +0.3 to −0.6 V vs SCE in acetonitrile at room temperature. Presumably the 2−/1− redox couple for **3b** is more positive-shifted and will appear above +0.3 V vs SCE when compared to the 3−/2− redox shift in the singly NH···S hydrogen-bonded model complexes as described above.

Table 7 also lists the electrochemical data obtained by the cyclic voltammograms in acetonitrile of singly and doubly NH···S hydrogen-bonded [2Fe-2S] complexes. The singly NH···S hydrogen bonded complexes have quasi-reversible redox couples of 3−/2− oxidation states at −0.90 V vs SCE for $(NEt_4)_2[Fe_2S_2(S\text{-}2\text{-}CH_3CONHC_6H_4\}_4]$ (**4a**), −0.94 V for $(NEt_4)_2[Fe_2S_2(S\text{-}2\text{-}t\text{-}BuCONHC_6H_4\}_4]$ (**5a**), and −0.80 V for $(NEt_4)_2[Fe_2S_2(S\text{-}2\text{-}CF_3CONHC_6H_4\}_4]$ (**6a**) and contribute to the positive shift of the redox potential by 0.1−0.24 V from that (−1.04 V vs SCE) of $[Fe_2S_2(SC_6H_5)_4]^{2-}$.[18] The substitution of the highly electron-withdrawing acyl group in the amide, e.g., $CF_3$, induces a positive-shifted redox potential (−0.80 V vs SCE) in acetonitrile. The electron-withdrawing groups in the amide moiety strengthen the NH···S hydrogen bond to result in a more positively shifted redox potential. The electrochemical data for singly NH···S hydrogen-bonded complexes show the lower reversibility in the 3−/2− redox couple compared with that of $[Fe_2S_2(SC_6H_5)_4]^{2-}$.

The doubly NH···S hydrogen-bonded complexes show a large redox potential shift by 0.25 V to +0.45 V from that of $[Fe_2S_2(SC_6H_5)_4]^{2-}$. The complex having the strongest NH···S bonding, **6b**, shows an extremely positive-shifted value at −0.59 V vs SCE beyond that of the native ferredoxin redox potential. The doubly NH···S hydrogen-bonded complexes exhibit a lower reversibility of the 3−/2− redox couple, showing a higher reactivity of the reduced state. The reduced state of the model complexes is kinetically unstable whereas the NH···S hydrogen bond in iron−sulfur proteins has been theoretically considered to thermodynamically stabilize the reduced state.[47]

**Ligand Exchange Reaction by Benzenethiol.** The UV−visible absorption spectra of a mixture of excess benzenethiol and a single NH···S hydrogen-bonded ferredoxin model complex, $(NEt_4)_2[Fe_4S_4(S\text{-}2\text{-}CH_3CONHC_6H_4)_4]$ (**1a**), were measured in acetonitrile at room temperature. The ligand exchange reaction readily occurs with the addition of 200 equiv of benzenethiol. A complete ligand exchange reaction has thus been established to give a clear absorption maximum at 445 nm for alkanethiolate model complexes, e.g., $(NEt_4)_2[Fe_4S_4(SCH_2C_6H_5)_4]$ in acetonitrile[3,18,24,48] and denatured ferredoxins in 4/1 v/v hexamethylphosphoramide/water solution, e.g., *C. pasteurianum* ferredoxin.[49,50]

On the other hand, in the case of the doubly NH···S hydrogen-bonded complex, $(PPh_4)_2[Fe_4S_4\{S\text{-}2,6\text{-}(CH_3CONH)_2C_6H_3\}_4]$ (**1b**), over 80% of the original thiolate still remains coordinated upon addition of an excess of 200 equiv of benzenethiol as evidenced by the absorption maximum at 445 nm. The results clearly indicate that the double NH···S hydrogen bond prevents the ligand exchange reaction.

Similar results were obtained with the $^1$H NMR titration. The ligand exchange reaction with benzenethiol was monitored by the $^1$H NMR spectra of a mixture of $(PPh_4)_2[Fe_4S_4\{S\text{-}2,6\text{-}(CH_3CONH)_2C_6H_3\}_4]$ and thiophenol (1:200 mol ratio) in acetonitrile-$d_3$. The rate of the ligand exchange reaction seems to slow due to the steric effect around the thiolate. When 200 equiv of benzenethiol is similarly added for the ligand exchange reaction to $(NEt_4)_2[Fe_4S_4(S\text{-}2,4,6\text{-}i\text{-}Pr_3C_6H_2)_4]$, the reaction was completed in 30 min. The fast reaction implies that the bulky alkane groups around the thiolate sulfur atom do not inhibit the exchange kinetically. Although two isopropyl groups at the 2,6-positions seem to cover the sulfur atom as indicated by the crystal structure reported for $(NEt_4)_2[Fe_4S_4(S\text{-}2,4,6\text{-}Me_3C_6H_2)_4]$,[30] the ligand exchange occurs rapidly. In the case of $(NEt_4)_2[Fe_4S_4(S\text{-}p\text{-}NO_2C_6H_4)_4]$ having higher acidity compared with that of the original benzenethiol, the ligand exchange reaction proceeds by 75% under the same conditions. The $^1$H NMR results of $(PPh_4)_2[Fe_4S_4\{S\text{-}2,6\text{-}(CH_3CONH)_2C_6H_3\}_4]$ indicate only 16% of the exchange with the addition of 200 equiv of benzenethiol. Holm et al. have already reported that the ligand exchange reaction is promoted with the increase in the acidity of added thiol. Thus, the rapid ligand exchange reaction was realized by the addition of *p*-nitrobenzenethiol to $(NEt_4)_2[Fe_4S_4(S\text{-}t\text{-}Bu)_4]$.[24,51]

The addition of an excess of benzenethiol (50 equiv) to a **4a** solution results in complete disappearance of these absorption maxima and shows the typical absorption maximum at 490 nm corresponding to the absorption maximum of $[Fe_2S_2(SC_6H_5)_4]^{2-}$.[18] A similar ligand exchange reaction proceeds to completion under these conditions as reported for alkanethiolate ferredoxin model complexes and denatured plant-type or adrenodoxin ferredoxins.[18,49,52]

The ligand exchange reaction was examined by the addition of excess benzenethiol (50 equiv) to an acetonitrile solution of **5b** at room temperature. The ligand exchange reaction does not proceed under these conditions as well as in the case of doubly NH···S hydrogen-bonded [4Fe-4S] model complexes. Two other complexes (**4b** and **6b**) also do not react with 50 equiv of benzenethiol. As described above, a singly NH···S hydrogen-bonded complex, e.g., **5a**, completely exchanges under the same conditions to give $[Fe_2S_2(SC_6H_5)_4]^{2-}$. Thus, the

(47) Noodleman, L.; Baerends, E. J. *J. Am. Chem. Soc.* **1984**, *106*, 2316.
(48) Bobrik, M. A.; Que, L., Jr.; Holm, R. H. *J. Am. Chem. Soc.* **1974**, *96*, 285.
(49) (a) Gillum, W. O.; Mortenson, L. E.; Chen, J.; Holm, R. H. *J. Am. Chem. Soc.* **1977**, *99*, 584. (b) Que, L., Jr.; Holm, R. H.; Mortenson, L. E. *J. Am. Chem. Soc.* **1975**, *97*, 463.
(50) Averill, B. A.; Bale, J. R.; Orme-Johnson, W. H. *J. Am. Chem Soc* **1978**, *100*, 3034.
(51) Dukes, G. R.; Holm, R. H. *J. Am. Chem. Soc.* **1975**, *97*, 528.
(52) Averill, B. A.; Orme-Johnson, W. H. In *Metal Ions in Biological Systems*; Sigel, H., Ed.; Marcel Dekker Inc.: New York, 1978; Vol. 7, p 127.

present doubly NH···S hydrogen-bonded [2Fe-2S] complexes are protected from the ligand exchange reaction as well as [4Fe-4S] model complexes.

## Discussion

**Formation of an NH···S Hydrogen Bond.** The X-ray crystallographic analysis of **1b** revealed the two amide NH groups within 3 Å of the sulfur atom as well as the presence of single and double NH···S hydrogen bonds in the native ferredoxins.[1,2] For example, the amide NH groups in *Peptococcus aerogenes* ferredoxin are directed to the cysteine thiolate sulfur atoms with a short N···S distance within 3.0−3.5 Å.[46] Recently, a careful study of the resonance Raman spectra of *P. aerogenes*, *B. thermoproteolyticus*, and *Azotobacter vinerandii* also indicated the existence of NH···S hydrogen bonds.[53]

The presence of the NH···S hydrogen bond was established by the IR spectra of $(NEt_4)_2[Fe_4S_4(S\text{-}2\text{-}t\text{-}BuCONHC_6H_4)_4]$ and $(NEt_4)_2[Fe_4S_4\{S\text{-}2,6\text{-}(t\text{-}BuCONH)_2C_6H_3\}_4]$. The IR shifts ($\Delta\nu$(NH)) of the NH stretching in 75 $cm^{-1}$ for $(PPh_4)_2[Fe_4S_4(S\text{-}2\text{-}t\text{-}BuCONHC_6H_4)_4]$ and 63 $cm^{-1}$ for $(NEt_4)_2[Fe_4S_4\{S\text{-}2,6\text{-}(t\text{-}BuCONH)_2C_6H_3\}_4]$ indicate that both shifts of the two NH groups in the double NH···S hydrogen bond are shown on the average and the effect is saturated. These hydrogen bond strengths estimated by the IR shifts are relatively weak as speculated for the NH···S hydrogen bonding in $(NMe_4)_2[Fe_4S_4(Z\text{-}\mathbf{cys}\text{-}Gly\text{-}Ala\text{-}OMe)_4]$ and $[(n\text{-}Bu)_4N]_2[Fe_4S_4(Z\text{-}\mathbf{cys}\text{-}Gly\text{-}NHC_6H_4\text{-}p\text{-}X)_4]$,[5,7] when compared with that of an ordinary NH···O═C hydrogen bond. Similar shifts have been observed for tetrahedral $[Co^{II}(S\text{-}2\text{-}t\text{-}BuCONHC_6H_4)_4]^{2-}$ (108 $cm^{-1}$)[54] and square-pyramidal $[Mo^{V}O(S\text{-}2\text{-}t\text{-}BuCONHC_6H_4)_4]^{-}$ (59 $cm^{-1}$)[35] as well as in recent data for $Mo[HB(Me_2pz)_3(NO)(SR)_2$,[55] but a relatively large shift (163 $cm^{-1}$) was found for $[Cu^{I}(S\text{-}2\text{-}t\text{-}BuCONHC_6H_4)_3]^{2-}$ [36] which is larger than the general intermolecular NH···O═C hydrogen bond in the solid state. Thus, the intramolecular NH···S hydrogen bond in ferredoxin model complexes with 2-(acylamino)benzenethiolate and 2,6-bis(acylamino)benzenethiolate ligands is rather weak although the designed ligands have a different N−H−S angle (∼110°) from that observed for a linear N−H−S angle (∼180°) in native ferredoxins.[1,2] Thus, alkanethiolate is similar to Cys thiolate in forming a stronger NH···S hydrogen bond than arenethiolate as pointed out by Walters et al.[55]

Interestingly, the NH···S hydrogen bond forms only between amide NH and thiolate sulfur atoms but not between the NH and disulfide sulfur atoms as shown by the comparison of the IR results. The absence of the NH···S hydrogen bond was shown by the crystal structure of bis{2,6-bis(pivaloylamino)-phenyl} disulfide, even though the two amide NH groups are directed to the sulfur atom.[34]

The blue shift of an absorption maximum in the region of 400−420 nm, characteristic of ferredoxin model complexes, also supports the presence of the NH···S hydrogen bond. The absorption in this region has been theoretically proposed to be associated with a charge transfer due to the transition from bonding Fe−S to antibonding Fe−S* (S* = inorganic sulfide).[43] The NH group interacting with the occupied bonding Fe−S orbital contributes to lowering of the energy level. Then an increasing energy gap between the hydrogen-bonded Fe−S and unaltered Fe−S* energy levels leads to the blue shift.

The characteristic absorption maximum appears around 400−420 nm as well as that of $[Fe_4S_4(S\text{-}2,4,6\text{-}Me_3C_6H_2)_4]^{2-}$, which has been reported to give a maximum at 409 nm in DMF and to have the hindered $\pi$-conjugated structure with a similar steric congestion due to two bulky methyl groups at the 2,6-positions.[30] The blue shift of the characteristic absorption maximum occurs upon introduction of an electron-withdrawing group ($CF_3$) in the amide acyl group. A similar effect through the NH···S hydrogen bond was found in $[(t\text{-}Bu)_4N]_2[Fe_4S_4(Z\text{-}\mathbf{cys}\text{-}Gly\text{-}NHC_6H_4\text{-}p\text{-}X)_4]$.[7] The amide NH of the anilide enhanced by an electron-withdrawing *p*-substituent (X) stabilizes the hydrogen bond. Therefore, it is likely that the formation of double NH···S hydrogen bond in native ferredoxins also contributes to the blue shift.

In the case of plant-type [2Fe-2S] ferredoxins, the presence of an NH···S hydrogen bond between the amide proton of the peptide chain and the sulfur atom coordinating to the Fe(III) ion has been detected by the X-ray crystal structure,[13,14] $^1H$ NMR spectroscopic,[15] and resonance Raman spectroscopic analyses.[16] The X-ray analysis indicates that most of the single NH···S hydrogen bond and the double NH···S hydrogen bonds converge on one of the two Fe(III) ions in the [2Fe-2S] cluster.

The direct evidence for the formation of the NH···S hydrogen bond is provided by the IR shift of the amide $\nu$(NH) band. $(NEt_4)_2[Fe_2S_2(S\text{-}2\text{-}t\text{-}BuCONHC_6H_4)_4]$ (**4b**) exhibits the shifts of 68 $cm^{-1}$ in the amide $\nu$(NH) and of 5 $cm^{-1}$ in the amide $\nu$(CO) band from those of the non-hydrogen-bonded NH and CO bands of the corresponding disulfide. The slightly smaller shift, compared with that (75 $cm^{-1}$) of $(NEt_4)_2[Fe_4S_4(S\text{-}2\text{-}t\text{-}BuCONHC_6H_4)_4]$, shows the presence of the relatively weak NH···S hydrogen bond.

The X-ray crystal structure of $(NEt_4)_2[Fe_2S_2\{S\text{-}2,6\text{-}(t\text{-}BuCONH)_2C_6H_3\}_4]$ (**5b**) indicates that all amide NH groups are directed to the neighboring sulfur atoms and form four sets of double NH···S hydrogen bonds in the solid state. The IR shifts of the $\nu$(NH) and $\nu$(CO) bands in **5b** from those in the corresponding disulfide are 66 and 20 $cm^{-1}$, respectively. The results indicate that the average strength of each of the doubly NH···S hydrogen bonds is weaker than that of the single hydrogen bond in **5a**. At present it is difficult to compare the accurate strengths of the double NH···S hydrogen bonds with that of the single NH···S hydrogen bond because of no information in the crystal structure of the sulfur geometry in any singly hydrogen-bonded [2Fe-2S] complex.

**Electrochemical Function of NH···S Hydrogen Bond.** The contribution of the NH···S hydrogen bond to the positive shift in redox potential was first proposed for native ferredoxins by Carter and his co-workers on the basis of the comparison of the redox potentials and their structures between *P. aerogenes* bacterial ferredoxin and *Chromatium vinosum* high-potential iron−sulfur protein.[11] The chemical roles have been experimentally demonstrated using oligopeptide model complexes having a $\beta$-turn-like structure that is preferable for the formation of the NH···S hydrogen bond in a less polar organic solvent, e.g., dichloromethane.[5,11]

The effect of polar environments around the cluster is significant for changing the redox potential as has been theoretically pointed out for ferredoxin model complexes[8] and experimentally demonstrated in native and denatured ferredoxins.[4] Similar dependence on the basicity of the solvent has been found in synthetic model [4Fe-4S] complexes.[9,56]

The single and double NH···S hydrogen bonds in the simple model complexes definitely contribute to the positive shift of the redox potential in the $[Fe_4S_4(SAr)_4]^{3-}/[Fe_4S_4(SAr)_4]^{2-}$

(53) Backes, G.; Mino, Y.; Loehr, T. M.; Meyer, T. E.; Cusanovich, M. A.; Sweeny, W. V.; Adman, E. T.; Sanders-Loehr, J. *J. Am. Chem. Soc.* **1991**, *113*, 2055.
(54) Ueyama, N.; Okamura, T.; Nakamura, A. *J. Chem. Soc., Chem. Commun.* **1992**, 1019.
(55) Huang, J.; Ostrander, R. L.; Rheingold, A. L.; Leung, Y.; Walters, M. A. *J. Am. Chem. Soc.* **1994**, *116*, 6769.
(56) Blonk, H. L. Ph.D. Thesis, Leiden University, 1991.

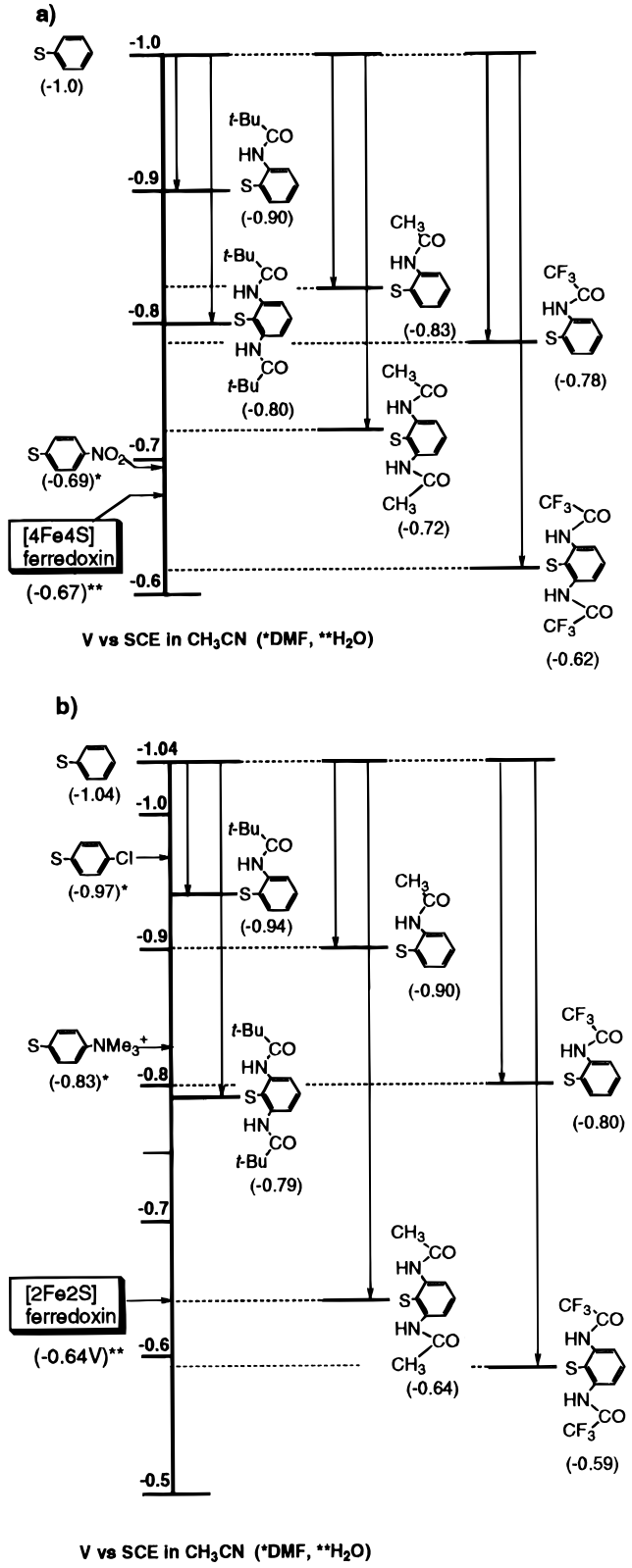


**Figure 6.** Additivity of the redox potential depending on the number of NH···S hydrogen bonds for (a) [4Fe-4S] ferredoxin model complexes and (b) [2Fe-2S] ferredoxin model complexes, compared with those of the reported arenethiolate model complexes[18] and native [4Fe-4S] and [2Fe-2S] ferredoxins.[66,67]

couple. The dependence of the redox potentials of various model complexes on the number and the strength of NH···S hydrogen bonds is illustrated in Figure 6a. Additivity in the redox potential between single and double NH···S hydrogen bonds is found. Previously we have discussed the limitation of the positive shift by the single NH···S hydrogen bond of the neutral amide group to approach −0.8 V vs SCE for cysteine-containing peptide model complexes in a less polar organic solvent.[7] The present simple model complexes having a single NH···S hydrogen bond similarly exhibit similar values, e.g., −0.83 V vs SCE for $[Fe_4S_4(S\text{-}2\text{-}CH_3CONHC_6H_4)_4]^{2-}$ and −0.78 V vs SCE for $[Fe_4S_4(S\text{-}2\text{-}CF_3CONHC_6H_4)_4]^{2-}$.

The observed shift due to the double NH···S hydrogen bonds, e.g., $[Fe_4S_4\{S\text{-}2,6\text{-}(CF_3CONH)_2C_6H_3\}_4]^{2-}$ (−0.62 V vs SCE in acetonitrile), is larger than that (−0.69 V in DMF) of $[Fe_4S_4(S\text{-}p\text{-}NO_2C_6H_4)_4]^{2-}$.[3] Holm and his co-workers have demonstrated that the electron-withdrawing *p*-substituent of benzenethiolate has an effect on the shift of the redox potential of $[Fe_4S_4(SAr)_4]^{2-/3-}$.[3,57] In native ferredoxins, the peptide amide groups around the metal sites exert an electronic effect not only on the carbonyl groups but also on the thiolate groups. The electronic effect through the double NH···S hydrogen bonds is relatively large compared with those of the *p*-substituent on the arenethiolate. Studies of the electronic effect through the NH---S hydrogen bond are still required to explain the origin, whether it is due to electrostatic interaction or charge transfer interaction.

In the case of native ferredoxins, an $(Fe_4S_4)^{2+}$ cluster has an asymmetric structure caused by the number of NH···S hydrogen bonds as shown in the crystallographically analyzed active center (Figure 1) of *P. aerogenes* ferredoxin.[1] Our results strongly suggest that a one-electron reduction to the 3- state in native ferredoxin occurs on one of the Fe ions having the double NH···S hydrogen bonds.

The double NH···S hydrogen bonds also contribute to the positive shift of the 2−/1− redox couple as shown in the electrochemical results for $(NMe_4)_2[Fe_4S_4\{S\text{-}2,6\text{-}(CF_3CONH)_2C_6H_3\}_4]$, which is relatively stable in air, resisting the fast one-electron oxidation by molecular dioxygen and the successive decomposition. The observed remarkable inertness to air is ascribed to the positive shift of the 2−/1− redox couple over +0.3 V vs SCE, although the 1− state obtained by one-electron oxidation is kinetically unstable as shown in the above electrochemical results. Native bacterial ferredoxins, e.g., *B. thermoproteolyticus* ferredoxins, have been known to be stable in air in aqueous solution but unstable in the denatured form. In the case of ferricyanide oxidation of *C. acidiurici* ferredoxin, only the 1− species is obtainable as a superoxidized form in small amounts.[58] Our present results suggest that the positive shift of the 2−/1− redox potential beyond +0.3 V vs SCE induces resistance to air oxidation.

In the case of [2Fe-2S] ferredoxin model complexes, the NH···S hydrogen bond contributes to the positive shift of the $[Fe_2S_2(SAr)_4]^{3-/2-}$ redox potential. The shift is proportional to the number of hydrogen bonds as shown in Figure 6b. Furthermore, the redox potential (−0.59 V vs SCE) of $(NEt_4)_2[Fe_2S_2\{S\text{-}2,6\text{-}(CF_3CONH)_2C_6H_3\}_4]$ having the strongest NH···S hydrogen bonding is beyond that of native plant-type ferredoxins. Of course, synthetic model complexes with benzenethiolate having an electron-withdrawing *p*-substituent, e.g., −CN or $-N^+Me_3$, have demonstrated a similar shift.[18] Here, it is emphasized that the amide NH group directing toward the thiolate sulfur functions in the formation of the NH···S hydrogen bond although the amide acts as a totally neutral group as providing a small Hammett $\sigma_p$ value (0.02) in the *p*-substituted aromatic compounds.[28]

In the active center of plant-type [2Fe-2S] ferredoxins, the single NH···S hydrogen bond and the double NH···S hydrogen

(57) Holm, R. H. *Acc. Chem. Res.* **1977**, *10*, 427.
(58) Sweeney, W. C.; Bearden, A. J.; Rabinowitz, J. C. *Biochem. Biophys. Res. Commun.* **1974**, *59*, 188.

bonds converge on one of the two Fe(III) ions in the [2Fe-2S] cluster. Presumably the $FeS_4$ core having the NH···S hydrogen bonds is easily reduced in a one-electron reduction as discussed for the positive shift in bacterial ferredoxins.

**Protection of the $(Fe_4S_4)^{2+}$ or $(Fe_2S_2)^{2+}$ Core by Double NH···S Hydrogen Bonds from Ligand Exchange Reaction.** The thiolate substitution reactions of alkanethiolate,[3,24,51] oligopeptide,[59] and various denatured [4Fe-4S] ferredoxins[49,60−62] have been studied extensively. The promotion of the core extrusion has been demonstrated with the addition of benzenethiol derivatives having higher acidity. Although the lowering of p$K_a$ due to the electron-withdrawing effect of the *p*-substituent in benzenethiol derivatives is known,[63] only a weak electronic effect of the two amide groups at the 2,6-positions of the benzene ring is expected because of the small Hammett $\sigma_p$ constant (−0.02).[28] Thus, a local interaction between the sulfur atom and amide NH upon NH···S hydrogen bonding significantly contributes to the stabilization of the thiolate against core extrusion. Of course, the lowering of p$K_a$ by the NH···S hydrogen bond will also occur for the one or two amide-substituted benzenethiols at the *o*- or *o*,*o*′-positions. Preliminary measurements of p$K_a$ values for 2-*t*-$BuCONHC_6H_4SH$ and 2,6-(*t*-$BuCONH)_2C_6H_3SH$ indicate the shift of 1 p$K_a$ unit per one NH···S hydrogen bond in 14% poly(ethyleneglycol) lauryl ether aqueous micellar solution.[64]

Ferredoxin model complexes have been known to be unstable in molecular dioxygen but also to hydrolytic and oxidative decomposition on exposure.[65] Two groups have independently proposed a mechanism for the ligand exchange reactions including the protonation of the coordinated thiolate as an intermediate process.[51,65] The observed ease of ligand exchange reaction from $(NEt_4)_2[Fe_4S_4(S\text{-}2,4,6\text{-}i\text{-}Pr_3C_6H_2)_4]$ by benzenethiol indicates that the bulkiness around the thiolate sulfur atom does not affect the protonation rate. The ligand exchange reaction is presumably prevented by the strong Fe−S bond with the stabilization of the thiolate by the NH···S hydrogen bonding. Thus, the double NH···S hydrogen bond definitely contributes to thiolate complex formation by the somewhat large binding constant even with the totally neutral amide groups.

## Conclusions

The double NH---S hydrogen bond clearly contributes to the positive shift of redox potential in [4Fe-4S] and [2Fe-2S] ferredoxin model complexes. The amide NH groups without substituent effect at the *o*,*o*′-positions can affect the Fe−S and its core through the NH···S hydrogen bonds similar to that of an electron-withdrawing *p*-substituent in the benzenethiolate ring. The hydrogen bond is also responsible for the protection of the iron−sulfur cluster from protonation, followed by ligand exchange reaction when an excess of benzenethiol is added. The stabilization of the thiolate anion is ascribed to electrostatic or scalar type bonding of the locally polarized NH group to the sulfur atom even with the neutral amide groups.

Our present results for the ferredoxin model complexes strongly suggest that the neutral amide groups participating in the NH···S hydrogen bond also contribute to the positive shift of redox potential and is associated with the large binding constant in the active center of native bacterial and plant-type ferredoxins.

**Acknowledgment.** Support of this work by a Grant-in-Aid for Specially Promoted Research (No. 06101004) from the Ministry of Education, Science, and Culture of Japan as well as the financial assistance by the Ogasawara Science Foundation is gratefully acknowledged.

**Supporting Information Available:** Tables of non-hydrogen atom anisotropic thermal parameters, complete geometric data, and atomic coordinates and *B* values (21 pages). Ordering information is given on any current masthead page.

IC9604324

(59) Que, L., Jr.; Anglin, J. R.; Bobrik, M. A.; Davison, A.; Holm, R. H. *J. Am. Chem. Soc.* **1974**, *96*, 6042.
(60) Que, L., Jr.; Holm, R. H.; Mortenson, L. E. *J. Am. Chem. Soc.* **1975**, *97*, 463.
(61) Mortenson, L. E.; Gillum, W. O. *Meth. Enzymol.* **1980**, *69*, 779.
(62) Wong, G. B.; D. M. Kurtz, J.; Holm, R. H.; Mortenson, L. E.; Upchurch, R. G. *J. Am. Chem. Soc.* **1979**, *101*, 3078.
(63) Jencks, W. P.; Salvesen, K. *J. Am. Chem. Soc.* **1971**, *93*, 4168.
(64) Ueyama, N.; Yamada, Y.; Okamura, T.; Inohara, M.; Moriyama, S.; Ueno, T.; Nakamura, A. To be submitted for publication.
(65) Bruice, T. C.; Maskiewicz, R.; Job, R. *Proc. Natl. Acad. Sci. U.S.A.* **1975**, *72*, 4795.
(66) Tagawa, K.; Arnon, D. I. *Biochem. Biophys. Acta* **1968**, *153*, 166.
(67) Cammack, R.; Rao, K. K.; Bargeron, C. P.; Hutson, K. G.; Andrew, P. W.; Rogers, L. J. *Biochem. J.* **1977**, *168*, 205.